Analyst

ROYAL SOCIETY OF CHEMISTRY

TUTORIAL REVIEW

View Article Online
View Journal | View Issue

Cite this: *Analyst*, 2023, **148**, 487

Recent advances in colorimetric sensors based on nanozymes with peroxidase-like activity

Zhongmei Chi, * Qiong Wang and Jiali Gu*

Nanozymes have been widely used to construct colorimetric sensors due to their advantages of cost-effectiveness, high stability, good biocompatibility, and ease of modification. The emergence of nanozymes greatly enhanced the detection sensitivity and stability of the colorimetric sensing platform. Recent significant research has focused on designing various sensors based on nanozymes with peroxidase-like activity for colorimetric analysis. However, with the deepening of research, nanozymes with peroxidase-like activity has also exposed some problems, such as weak affinity and low catalytic activity. In view of the above issues, existing investigations have shown that the catalytic properties of nanozymes can be improved by adding surface modification and changing the structure of nanomaterials. In this review, we summarize the recent trends and advances of colorimetric sensors based on several typical nanozymes with peroxidase-like activities, including noble metals, metal oxides, metal sulfides/metal selenides, and carbon and metal–organic frameworks (MOF). Finally, the current challenges and prospects of colorimetric sensors based on nanozymes with peroxidase-like activity are summarized and discussed to provide a reference for researchers in related fields.

Received 10th November 2022,
Accepted 29th November 2022

DOI: 10.1039/d2an01850k

rsc.li/analyst

1. Introduction

Nanomaterials with sizes of 1–100 nm may possess unique chemical, optical and electrical properties.[1–3] Since the discovery of ferromagnetic nanoparticles through pioneering work in 2007,[4] a growing number of nanomaterials have attracted extensive research. Nanozymes refer to nanomaterials showing intrinsic enzyme-like catalytic activities. They exhibit the advantages of low-cost, high stability, and ease of modification, which are expected to be the direct surrogates of natural enzymes.[5–7] Furthermore, nanozymes are less sensitive to pH and temperature changes than natural enzymes, and thus generally lead to more robust analytical assays. Thus far, great efforts have been devoted to developing various nanozymes, such as noble metals,[8,9] metal oxides,[10,11] metal sulfides/metal selenides,[12,13] carbon materials[14,15] and

College of Chemistry and Materials Engineering, Bohai University, Jinzhou, Liaoning Province, 121013, P. R. China. E-mail: 980058161@qq.com

Zhongmei Chi

Zhongmei Chi received her BS degree (2016) in Chemistry at Liaoning Normal University and PhD degree (2021) in Analytical Chemistry at Northeast Normal University. She joined the College of Chemistry and Materials Engineering at Bohai University in 2021. Her current research interests are focused on the development of bioanalytical methods and biosensors to address challenging problems in bioanalytical, environmental and pharmaceutical analysis.

Qiong Wang

Qiong Wang received her BS degree (2013) in Chemistry at Anshan Normal University and PhD degree (2019) in Analytical Chemistry at Liaoning University. She joined the College of Chemistry and Materials Engineering at Bohai University in 2019. She is mainly engaged in the research work of electrical/photoelectric chemical detection and catalytic degradation, and establishes rapid and sensitive analysis and detection methods for organic pollutants and biological small molecules in the environment.

metal–organic frameworks (MOFs).[16–18] Various nanozymes have extremely broad application prospects in the fields of biosensing, immunoassay, and disease diagnosis.[19–21]

Very recently, nanozyme-based sensors have been widely applied in electrochemical,[22–24] chemiluminescence,[25–27] luminescence,[28–30] and colorimetric[31–33] detection. Compared with other sensors, colorimetric sensors based on color change analysis can directly or indirectly achieve qualitative and quantitative detection of the target causing color change that is visible through naked eye observation[34,35] or smartphone color readout device.[36,37] Due to the merits of quick response, low cost, and no requirement of sophisticated instruments and professional operators, colorimetric sensors as a novel strategy have drawn tremendous attention.[38–41] Thus, simple colorimetric assays-based nanozymes offer the unflinching biocatalytic potential for portable and inexpensive daily applications.

Nanozymes materials themselves show no light absorption properties in the constructed colorimetric sensors. After the introduction of a chromogenic substrate, nanozymes act as catalysts to catalyze the reaction of the substrate to trigger the light signal output, thus amplifying the signal as well as improving the sensitivity of colorimetric sensors.[42,43] The types of nanozymes currently reported include peroxidase,[44] oxidase,[45] catalase,[46] and superoxide dismutase.[47] Among them, peroxidase is the most widely investigated nanozyme.[48–50] For the peroxidase-mimetic system, nanozymes can efficiently catalyze the chromogenic substrates, such as 3,3′,5,5′-tetramethylbenzidine (TMB),[51] 2,2′-azino-bis-3-ethylbenzothiazoline-6-sulfonic acid (ABTS),[52] and *o*-phenylenediamine dihydrochloride (OPD),[4] to generate chromogenic products also accompanied by colorimetric signals in the presence of hydrogen peroxide (H_2O_2). The mechanism of catalytic color involves nanozymes decomposing the O–O bond of H_2O_2 into hydroxyl radicals ($^{\bullet}OH$) with high oxidative capacity and then generating $^{\bullet}OH$ that further oxidizes chromogenic substrates.

Earlier reviews on nanozymes mainly focused on the aspects of fluorescent and electrochemical sensors. To date, almost few reviews have concentrated on nanozyme-based colorimetric assays. As a result, this review aims to highlight the recent advancements and applications of colorimetric sensors based on nanozymes with peroxidase-like activity, including noble metals, metal oxides, metal sulfides/metal selenides, carbon materials, and MOFs. Finally, we discuss the challenges faced in the nanozyme-based colorimetric sensors and look forward to the future development directions.

Jiali Gu

Jiali Gu received her BS degree (2003) in Chemistry at Liaoning University and PhD degree (2021) in Analytical Chemistry at Northeast University. She joined the College of Chemistry and Materials Engineering at Bohai University in 2006. She mainly focuses on the interaction mechanism between exogenous small molecules and biological macromolecules.

2. Metal-based nanozymes

The noble metal nanomaterials are stable and show catalytic performance similar to peroxidase. Their catalytic activity is mainly achieved by surface adsorption and rapid electron transfer. Thus, metal nanomaterials, including noble metals, transition metals, and alloys-based nanoparticles/nanoclusters (NPs/NCs) have been reported as enzyme mimics. For instance, gold (Au), platinum (Pt), palladium (Pd), and copper (Cu) NPs/NCs with intrinsic peroxidase-like activity have been successfully used in the colorimetric determination of Ag^{+}, Hg^{2+}, glucose, H_2O_2, dopamine, and xanthine, *etc.*

2.1 Au-based nanozymes

In recent years, Au NPs have received more and more attention due to their simple preparation, good biocompatibility, and optoelectronic properties. In 2010, Jv Y. *et al.* discovered that positively charged Au NPs with peroxidase-like activity could be used to detect H_2O_2 and glucose.[53] Au NPs could catalyze the oxidation of TMB-H_2O_2, which turned the colorless solution to blue. Based on this, a colorimetric sensor based on Au NPs was developed for the detection of H_2O_2 and glucose, and the detection limits (LODs) were 0.5 μM and 4 μM, respectively.

Recently, paper-based sensors fabricated by modifying Au NPs on the paper have attracted considerable attention in improving colorimetric homogeneity and sensitivity.[54] For example, Han N. K. *et al.* reported an Au NP-based paper chip for colorimetric detection of Hg^{2+}.[55] The combination of Hg^{2+} and Au NPs formed an Au–Hg alloy, which stimulated the peroxidase-like activity of Au NPs. The chromogenic substrates TMB were oxidized to blue stain on the cellulose paper chip by Au–Hg alloy in the presence of H_2O_2, with a LOD of 30 μg L^{-1}. Subsequently, wicking pads (Whatman No. 1 filter paper) loaded with DNA-Au NPs were also developed to fabricate a paper device for colorimetric detection of Hg^{2+}.[56] DNA is an important substance that can control the peroxidase-like activity of various nanomaterials.[57] Thus, DNA-Au NPs could combine with Hg^{2+} to produce a more stable DNA-Au–Hg alloy for enhancing peroxidase-like activity. Besides, wicking pads can adsorb a large volume of Hg^{2+} solution, therefore the color signal was significantly enhanced, and the lower LOD was 10 nM.

In addition, due to their specific identification function and easy modification, aptamers are mainly exploited as identification, signal conversion, and signal amplification elements in the design of colorimetric sensors.[58] Recently,

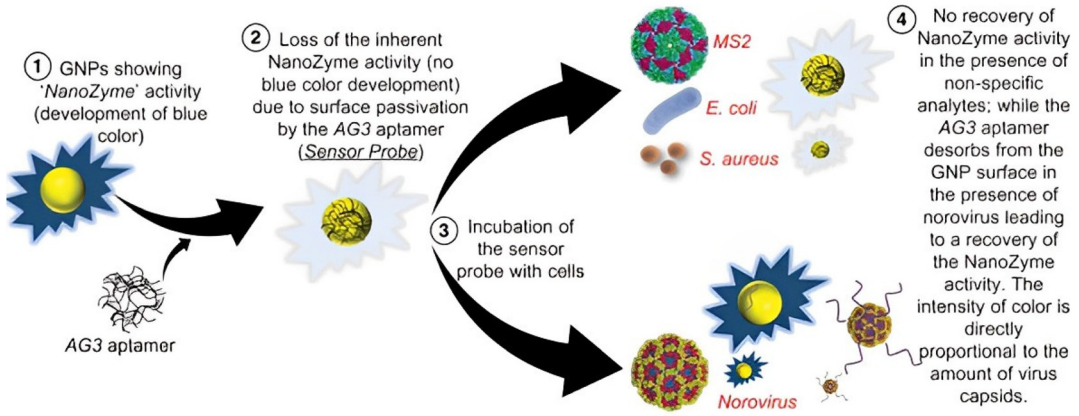

Fig. 1 Schematic diagram of the nanozyme aptasensor prepared by adapting Au NPs to norovirus aptamer.[62]

aptamer-based Au NP sensors have been used for competitive colorimetric analysis.[59–61] The aptamers will inhibit the intrinsic peroxidase-mimicking activity of Au NPs by simply adsorbing onto the Au NPs surface. However, when there was a target, the target–aptamer will leave the Au NPs surface due to the high affinity and specificity to the target. Therefore, Au NPs restored their peroxidase-like activity for catalyzing TMB to produce a blue color. For example, an Au NP-based nanozyme aptasensor was proposed for ultrasensitive colorimetric sensing of murine norovirus (Fig. 1). An aptasensor probe was prepared by combining Au NPs with the high target specificity of a murine norovirus aptamer, which produced a blue color in the presence of a norovirus target.[62] Similarly, other Au NP-based aptasensors were also used for colorimetric detection of *Pseudomonas aeruginosa*[63] and multiple diarrheic shellfish poisons.[64] More importantly, the peroxidase-like activity of Au NP-based aptasensors can be remarkably promoted by the hybridization chain reaction, enabling highly sensitive colorimetric detection of saxitoxin with a LOD as low as 42.46 pM.[65] Thus, Au NP-based colorimetric aptasensors will be a promising direction for colorimetric sensor research.

Although the enzymatic catalytic activity has been greatly improved, Au NP-based nanozymes still face the challenges of difficult recovery and reuse. Alle M. *et al. in situ* synthesized Au NPs@cationic cellulose nanofibrils (C.CNF) nanozymes using C.CNF-loaded positively charged Au NPs, which could be reused by casting into a film.[66] A sensitive colorimetric approach based on recyclable nanozymes was established for the detection of glucose in human serum with the help of the TMB substrate. Afterwards, the same group fabricated a reusable nanozyme *via* Au NPs immobilized on dialdehyde cellulose nanofibrils (DACNF).[67] Au NPs@DACNF was modified onto a paper sensor for the colorimetric detection of cholesterol with ABTS as a substrate. Cholesterol oxidase (ChOx) catalyzed the oxidation of cholesterol to 4-cholestene-3-one and H_2O_2, and the resulting H_2O_2 further oxidized colorless ABTS to blue products in the presence of Au NPs@DACNF nanozymes. A smartphone application was employed to visually record and analyze color changes (Fig. 2). Additionally, some materials, such as quantum dots (QDs),[68] β-cyclodextrin (β-CD),[69] polyoxometalates (POMs),[70] polyvinyl alcohol,[71] hydrogel,[72] cysteamine[73] and tannic acid[74] combined with Au NPs showed higher cata-

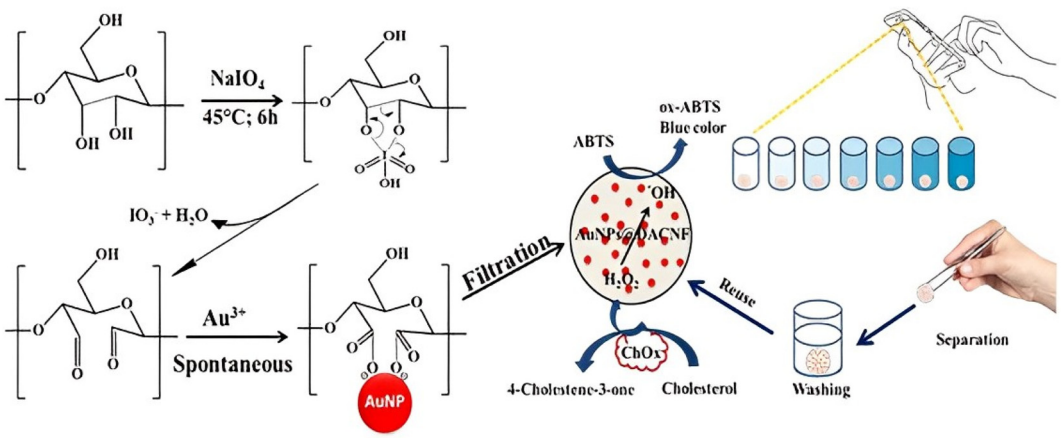

Fig. 2 Schematic illustration of the preparation of paper-based Au NPs@DACNF sensor and the colorimetric detection of cholesterol assisted by smartphone.[67]

lytic activity under neutral conditions, and were successfully utilized for colorimetric detection of metal ions and small biological molecules.

2.2 Pt-based nanozymes

In addition to Au nanomaterials, numerous investigations have proved that Pt nanomaterials can also be employed as peroxidase mimics for colorimetric assays. Compared with other metal-based nanozymes, Pt NPs possess much stronger activity for interacting with H_2O_2. However, due to the shortcomings of high polymerization cost and easy deactivation, the application scope of Pt NPs is greatly limited. To overcome these problems, Jin L. H. *et al.* prepared ultra-small Pt NCs for glucose analysis with the good catalytic ability and good biocompatibility *via* a one-pot hydrothermal approach.[75] Besides precisely controlling the size and morphology of Pt nanomaterials, the catalytic activity of peroxidase-like enzymes can also be enhanced by surface modification. Li W. *et al.* selected bovine serum albumin (BSA) as the stabilizing agent to synthesize Pt-based nanozymes.[76] BSA was regarded as an efficient template for the direct oriented growth of metal nanocrystals. BSA-stabilized Pt nanozymes, consisting of 57% Pt^0 y with an average diameter of 2.0 nm have high peroxidase-like activity. Hg^{2+} was determined by label-free colorimetric strategy, which mainly reduced the enzyme activity of Pt NPs through the interaction with Pt^0. This colorimetric sensor can detect Hg^{2+} in drinking water with a linear range of 0–120 nM and a LOD of 7.2 nM. Furthermore, the same group found that *N*-acety-L-cysteine (NAC) exhibited strong affinities to transition metal ions.[77] They adopted NAC as the nucleation template to synthesize Pt NCs. This colorimetric assay of heparin was achieved by the interactions among Pt NCs, heparin and the TMB substrate, with a LOD of 2×10^{-3} μg mL^{-1}. Such a colorimetric sensor has the advantages of high sensitivity, short sensing time, and is free of expensive instruments. In addition, nanozyme-linked immunoassays with Pt NPs offer a new platform for the colorimetric detection of parathion[78] and triazophos.[79]

2.3 Pd-based nanozymes

Fu Y. *et al.* developed Pd-based nanozymes that were utilized for the colorimetric detection of Ag^+.[80] The synthesized Pd-based nanozymes using reduced glutathione (GSH) exhibited a high affinity for transition metal ions. They first reported that Ag^+ can obviously inhibit the peroxidase-mimicking activity of Pd NPs. This inhibition was employed for highly sensitive colorimetric detection of Ag^+ and Ag NPs in an aqueous solution by using TMB as a chromogenic substrate. Subsequently, the same group was inspired by GSH-capped Pd NPs, and they once again developed, for the first time, oligonucleotide-stabilized Pd NPs for the colorimetric detection of biothiols, with LODs of as low as 3.7 nM and 4.3 nM for cysteine and homocysteine, respectively.[81] Thus, Pd-based nanozymes with simulated peroxidase-like activities show broad application prospects for quantitative colorimetric detection.

2.4 Alloy-based nanozymes

Due to the synergistic effect of alloy-based nanozymes, their catalytic activities are generally stronger than those of single-metal nanomaterials. Among the various alloy nanomaterials, Pt-based alloy nanozymes are considered strong candidates for colorimetric analysis. For instance, Sun YH and coworkers have synthesized Au_xPt_y nanozymes with high peroxidase mimicking activity.[82] They first reported DNA-stabilized bimetallic Au_xPt_y nanozymes for the colorimetric detection of biothiols using TMB as an indicator. Sun Y. *et al.* uniformly and rapidly grew Pt NPs on the surface of Au NRs using laser irradiation procedure.[83] The prepared Au/Pt nanorods (NRs) possessed enhanced peroxide-like activity and surface-enhanced Raman scattering (SERS) efficiency, which realized the high sensitivity colorimetric detection of H_2O_2, with a LOD of 0.04 μM. Very recently, CuPt nanozymes with powerful catalytic ability have been extensively investigated. Lu Y. *et al.* fabricated three-dimensional (3D) layered porous CuPt dendrites (HPPtCuDs) by electrochemical displacement and chemical dealloying.[84] Due to the electronic effect and geometric effect, HPPtCuDs showed enhanced peroxide-like activity, which was applied for colorimetric detection of H_2O_2 (Fig. 3). In addition, Wu L. L. *et al.* found that the catalytic performance of AgPt NCs could be inhibited by 3-mercaptopropionic acid (MPA), but could be recovered after catalyzed oxidation by Cu^{2+}. Therefore, they successfully proposed a sensitive colorimetric method for detecting Cu^{2+} *via* the TMB-H_2O_2 reaction system.[85] Nevertheless, only a small fraction of Pt atoms were exposed when Pt-based nanozymes were synthesized by traditional methods. Therefore, the content of Pt atoms involved in the catalytic reaction was low, giving rise to poor catalytic performance. To overcome this limitation, Panferov V. G. *et al.* developed a new approach for efficient and uniform distribution of Pt atoms on nanozymes surfaces.[86] Au core and Ag shell were applied to form Au@Ag NPs, and then the galvanic replacement of Ag with $PtCl_6^{2-}$ resulted in the formation of Au@Ag–Pt NPs.

Besides Pt-based alloy nanozymes, Au-based alloy nanozymes with peroxidase-like activity are also attracting significant interest in colorimetric assays. Singh S. *et al.* explored the peroxide potential of Pd@Au NRs.[87] The catalytic activity of Pd NPs dispersed on the surface of Au NRs was higher than that of Au NRs alone. Pd@Au NR-based nanozymes were employed for colorimetric sensing of malathion using OPD-H_2O_2 as substrates, with the lowest LOD of 60 ng mL^{-1}. The peroxidase-mimicking activity of Ag–Au-based nanozymes was also demonstrated for visual colorimetric assays. Liu H. *et al.* covalently cross-linked Hemin (Hem) onto melamine (MA) through an EDC-NHS chemical bond to prepare a Hem-MA polymer matrix.[88] MA-Hem/Au–Ag nanocomposites were fabricated by the bimetallic Au–Ag in-site mineralization into the Hem-MA polymer matrix (Fig. 4A). Moreover, the catalytic activity of complex enzymes obtained by combining MA-Hem/Au–Ag nanozymes with glucose oxidase (GOx) was investigated. As described in Fig. 4B, MA-Hem/Au–Ag-GOx complex enzymes

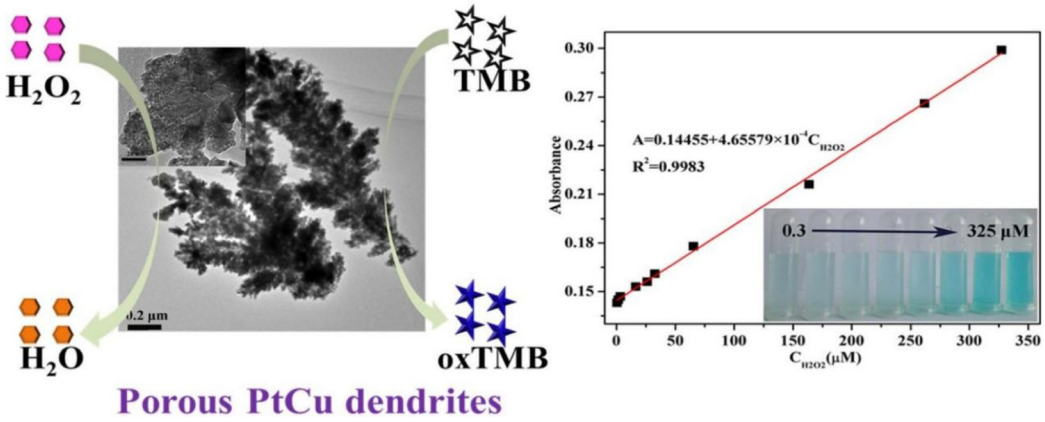

Fig. 3 Schematic diagram of HPPtCuDs catalysis of the classical peroxidase substrate TMB by H_2O_2 and linear calibration plot for H_2O_2 detection.[84]

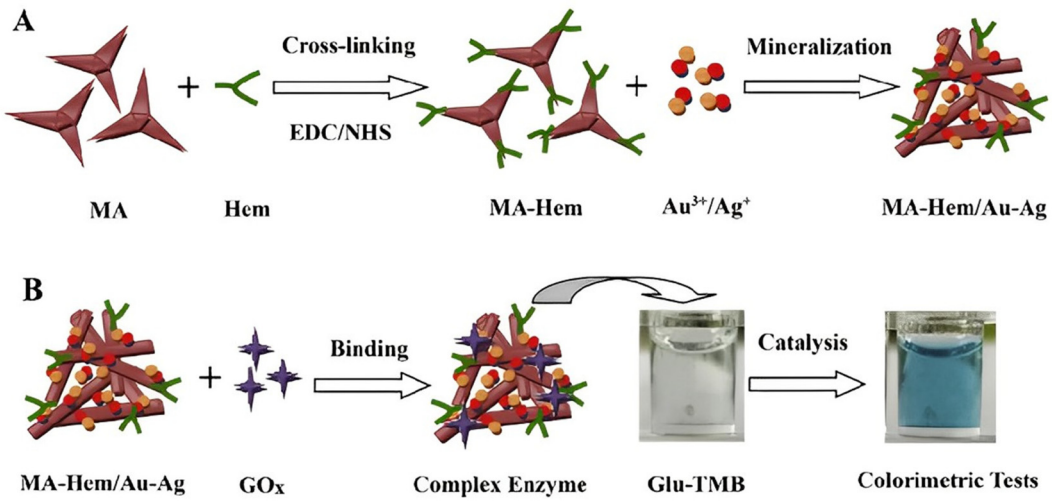

Fig. 4 Schematic diagram of (A) MA-Hem/Au–Ag nanozymes prepared by MA-Hem cross-linking and Au–Ag mineralization, and (B) complex enzymes obtained by MA-Hem/Au–Ag nanozymes attached with GOx for colorimetric detection of glucose.[88]

catalyzed the oxidation of glucose-TMB to generate a blue signal. Complex enzymes exhibited significantly-enhanced catalytic activity due to the introduction of the Au–Ag bimetallic into the Hem-MA polymer matrix. It could not only be functionalized into "nanowires" to accelerate electron transfer but also had high adsorption capacity and affinity for the substrates. Similarly, Fang H. *et al.* proposed a colorimetric nanozyme-linked immunosorbent assay (NLSA) based on Au@Ag NPs nanocomposites.[89] NLSA showed high sensitivity by M13 bacteriophage as a competing antigen assembled Au@Ag NPs for deoxynivalenol (DON) detection, with the LOD of 13.67 pg mL^{-1}.

3. Metal oxide-based nanozymes

Metal oxide nanomaterials are usually composed of transition metal oxide nanomaterials. The binding of such nanozymes to reaction substrates is usually accompanied by electron transfer and valence changes. Metal oxides nanozymes exhibiting peroxidase-like catalytic behavior possess the advantages of good stability, simple preparation process, and low cost, which have also been investigated for the colorimetric detection of various biomolecules, such as glucose, H_2O_2, and nucleic acids.

3.1 Fe_3O_4-based nanozymes

In 2007, Gao *et al.* first reported that Fe_3O_4 nanomaterials showed peroxidase-like performance.[4] Recently, a novel type of anti-aggregation nanozyme was synthesized containing Fe_3O_4 NPs immobilized monodispersed-porous SiO_2 microspheres (Fe_3O_4 NP@pSiO_2), which significantly enhanced the peroxidase-mimicking activity of Fe_3O_4.[90] Previous studies have indicated that SiO_2 can be grown in different NPs surfaces to form uniform core–shell nanostructures.[91,92] For the first time, Fe_3O_4 NP@pSiO_2 nanozymes were utilized to colorimetric determine human genomic DNA using OPD-H_2O_2 as sub-

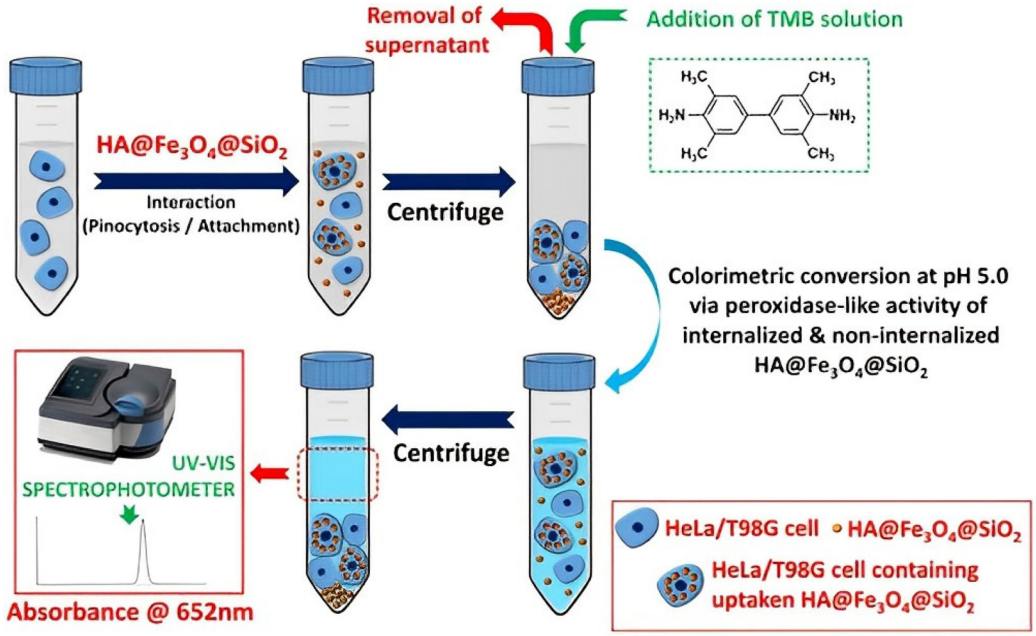

Fig. 5 A schematic diagram for colorimetric determination of HeLa and T98G cell concentrations based on the difference in peroxidase-mimicking activity of HA@Fe_3O_4@SiO_2 nanozymes.[93]

strates, and could also be applied for detecting other similar biological macromolecules. Subsequently, the same group selected an intracellular hyaluronic acid (HA) functionalized nanozyme as the ligand to obtain HA@Fe_3O_4@SiO_2 microspheres by carbodiimide activation.[93] A simple colorimetric protocol based on HA@Fe_3O_4@SiO_2 nanozymes against TMB as the substrate was applied for the determination of tumor cells, including human cervical cancer (HeLa) and primary brain tumor (T98G) cells (Fig. 5).

In addition, Yardimci B. *et al.* synthesized reusable and low-cost ethylenediamine (EDA)-modified Fe_3O_4 NPs in a one-pot reaction.[94] The EDA@Fe_3O_4 nanozyme colorimetric sensors were designed to detect TNT/tetryl *via* catalyzed H_2O_2 oxidation to produce a blue-colored complex from oxidized TMB. The principle of the colorimetric sensors was that TNT and tetryl caused fading of blue color by inhibiting the catalytic performance of EDA@Fe_3O_4 nanozymes. Inspired by the principle of complementary coloring harmonics, Su M. *et al.* designed a bisubstrate multi-colorimetric system based on polyethylene glycol (PEG)@Fe_3O_4 NPs. According to the hue circle, TMB and dopamine were chosen to form the complementary colors of blue and orange.[95] Thus, PEG@Fe_3O_4 NPs with peroxidase-like performance catalyzed the oxidation of TMB-dopamine for three-color threshold colorimetric detection of H_2O_2.

Although Fe_3O_4-based nanozymes colorimetry has been widely used in the field of biosensing, some limitations of nanozymes, such as the low catalytic ability and poor sensitivity to analytes remain unsolved. To address these shortcomings, multiple metal–metal oxide interfaces are good candidates for synergistic effects. Zeng's group rationally designed a Pd-Fe_3O_4 Janus nanozyme *via* a seed-mediated method.[96] Due to the synergistic effect of Pd and Fe_3O_4 in dumbbell-like nanostructures, the ultrasensitive colorimetric detection of biothiols was realized. Meanwhile, the same group established an innovative colorimetric fluoride (F^-) probe with high sensitivity and specificity based on AgPt-Fe_3O_4@SiO_2.[97]

3.2 CeO_2-based nanozymes

CeO_2 displays strong redox behavior and enzyme-mimetic characteristics ascribed to its excellent O_2 storage capacity and reversible valence switching between Ce(III) and Ce(IV). e Jiao X. *et al.* in 2012 reported that CeO_2 NPs possessed peroxidase-like activity;[98] how to improve their catalytic performance has become the focus of researchers. The current investigations demonstrated that surface functionalization and carrier loading can significantly improve the catalytic activity of CeO_2. Lian J. J. *et al.* successfully fabricated functionalized CeO_2 of perylene diimide (PDI) nanocomposites *via* a one-pot hydrothermal method.[99] The combination of PDI and CeO_2 maintained the excellent electron transfer ability of PDI and the strong redox ability of CeO_2. Therefore, a highly sensitive and selective colorimetric sensor based on PDI-CeO_2 nanocomposites was achieved for the detection of H_2O_2 and GSH, with LODs of 2.59 μM and 0.92 μM, respectively.

Furthermore, due to the synergistic effects of bimetallic oxides and enzymatic cascade reactions, the obtained CeO_2 has higher catalytic efficiency and stability. Chi M. Q. *et al.* prepared CeO_2/Co_3O_4/poly(3,4-ethylenedioxythiophene) (PEDOT) composite nanofibers using an electrospinning and calcination process, followed by a redox reaction.[100] They found that the enhanced peroxidase-mimicking activity of CeO_2/Co_3O_4/

PEDOT nanozymes was due to the synergistic interactions between multiple components. Therefore, a novel high-sensitivity colorimetric platform was established for the detection of H_2O_2 using CeO_2/Co_3O_4/PEDOT composite nanofibers. Liu M. *et al.* synthesized a CeO_2/GOx multi-enzyme complex *via* self-assembly.[101] In this cascade catalytic system, GOx catalyzed the oxidation of glucose to produce H_2O_2, while CeO_2 immediately degraded H_2O_2 with minimal diffusion (Fig. 6). Such an enzyme cascade reaction-based CeO_2/GOx hybrid nanocomplex system was employed to establish a colorimetric sensor with high selectivity and sensitivity for glucose detection.

Recently, the design and development of CeO_2 nanozyme-based logic gates for colorimetric analysis have sparked extensive research efforts.[102] Chishti B. *et al.* successfully integrated two and a three-input regulated AND logic circuit, and established a visual colorimetric sensor for the detection of melamine at acidic (4.5) and neutral (7.4) pH.[103] The constructed logic gate sensor based on the intrinsic peroxidase-like activity of CeO_2 NRs displayed a high affinity for melamine, producing outstanding visual output on a logic platform of TMB/H_2O_2 (Fig. 7). The developed sensor was successfully applied for the detection of melamine in raw milk and infant formula with picomolar sensitivity.

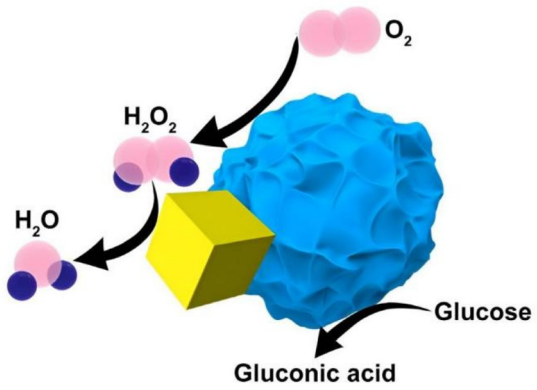

Fig. 6 Cascade reaction diagram of CeO_2/GOx multi-enzyme complex catalyzed oxidation of glucose.[101]

3.3 MnO_2-based nanozymes

MnO_2 nanosheets as typical nanozymes possess appealing peroxidase-mimicking performance. Research on the peroxidase-like activity of MnO_2 NPs has gradually deepened, and their catalytic activity can be improved by surface modification and loading. For example, Li Y. R. *et al.* established an immunosensor based on MnO_2 NPs AND tyramine-triggered reaction for the amplification detection of alpha-fetoprotein (AFP) in human serum samples.[104] Briefly, superparamagnetic beads (MBs)-Ab_1 binding can specifically capture AFP in the sample solution. Then, a sandwich immune complex was formed with Ab_2-MnO_2 NPs through specific antibody–antigen interaction. Upon the introduction of H_2O_2, multiple MnO_2 NPs can be conjugated to the surface of the immune complex through a tyramine-mediated reaction, resulting in signal amplification. Accordingly, MnO_2 NPs with peroxidase-like activity can catalyze TMB from colorless to blue with repeated cycles of catalytic reactions.

Likewise, Guan's group developed a colorimetric immunoassay based on MnO_2 NRs for the detection of human chorionic gonadotropin (HCG).[105] They synthesized MnO_2 NRs with outstanding peroxidase-like activity using a hydrothermal method using EDTA as a template. The MnO_2 NRs were first immobilized in the chitosan matrix of the BSA-modified 96-well plastic microplates, and then the microplates were further modified by streptavidin and biotinylated β-HCG anti-

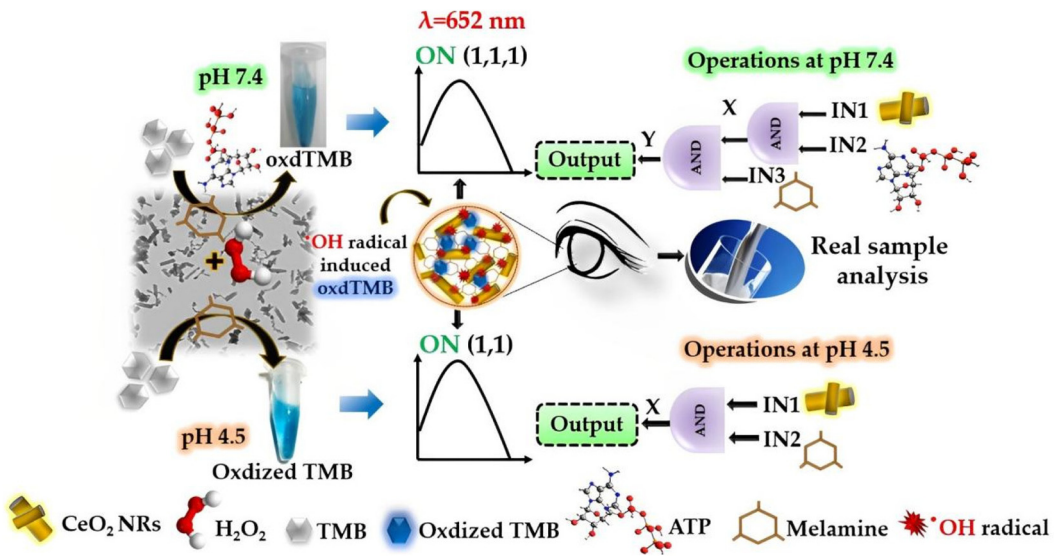

Fig. 7 Schematic illustration of the logic operation mechanism for melamine detection based on peroxidase-like activity of CeO_2 NRs at acidic (4.5) and neutral (7.4) pH.[103]

bodies. In the presence of HCG antigen, the specific recognition between HCG-antibodies on the sensing platform inhibited the peroxidase-like activity of MnO_2 NRs through the steric hindrance effect. Therefore, based on this principle, as the HCG concentration was increased, the blue color generated by MnO_2 NRs catalyzing TMB-H_2O_2 substrate gradually faded, which allowed for quantitative colorimetric sensing of HCG.

Although this review introduced the aforementioned metal oxides with peroxidase-like activity, the research is not limited to these. Other metal oxide-based nanozymes, such as copper (I) oxide (Cu_2O),[106] cobaltous oxide (CoO),[107] molybdenum oxide (MoO_3)[108] and tricobalt tetraoxide (Co_3O_4)[109] also have intrinsic peroxidase-like characteristics, forming a rich metal oxide-based nanozyme systems. These novel metal oxide-based nanozyme colorimetric platforms have the potential to be applied for sensing H_2O_2, glucose, acid phosphatase, and glyphosate.

4. Metal sulfide/metal selenide-based nanozymes

4.1 Metal sulfide-based nanozymes

A variety of metal sulfide-based nanomaterials have been widely used and studied because of their special structures and characteristics. Among them, the use of molybdenum disulfide (MoS_2) with two-dimensional (2D) graphene-like layered materials have aroused remarkable interest in colorimetric assays. Lin T. R. *et al.* discovered that MoS_2 nanosheets possessed intrinsic peroxidase-like properties, which can catalyze the oxidation of TMB by H_2O_2, resulting in a color reaction.[110] Studies have shown that the surface modification of nanozymes can affect their catalytic performance. Based on this, Xian Z. Q. *et al.* formed a flower-like polymer MoS_2@$CoFe_2O_4$ nanozyme based on $CoFe_2O_4$ modified with MoS_2 for the colorimetric detection of cysteine (Cys) and GSH.[111] TMB and H_2O_2 as substrates, MoS_2@$CoFe_2O_4$ catalyzed oxidation of TMB to generate a blue color. The competition of TMB with Cys or GSH led to the gradual fading of the blue color of oxidized TMB with the increase of Cys or GSH content. It has been found that the favorable dispersion of MoS_2 can reduce the aggregation effect of ferrite. Meanwhile, when interacting with ferrite, the peroxidase-mimicking activity of MoS_2@$CoFe_2O_4$ was 4.4-fold and 1.8-fold to that of MoS_2 and $CoFe_2O_4$, respectively.

Inspired by the above work, Feng L. P. *et al.* first simply doped MoS_2 nanosheets with Fe element *via* a one-pot hydrothermal route, obtaining a highly superior peroxidase-like catalytic Fe-MoS_2 nanozymes (Fig. 8).[112] Thus, Fe-MoS_2 nanosheet-based colorimetric strategy realized the detection of glucose with satisfactory sensitivity. Except for Fe-based doping, Prussian blue NPs (CPBNPs) or other metals (*i.e.*, Au, Ag, and Pd) NP hybridized MoS_2 nanosheets can also increase the peroxidase-mimicking activities of MoS_2. Zhu Z. Q. *et al.* prepared MoS_2-CPBNPs nanozymes to present a probe for colorimetric detection of dopamine (DA), with a LOD of 0.09 μM.[113] As expected, MoS_2-CPBNPs nanozymes showed superior peroxidase-like activity and catalyzed TMB to produce a blue product and $^{\bullet}OH$ in the presence of H_2O_2. While adding DA, the color of the solution gradually faded and the adsorption strength decreased with the consumption of $^{\bullet}OH$. Moreover, a series of polypyrrole (PPy)@MoS_2-based nanozymes deposited on three typical metal NPs (Au, Ag, and Pd NPs) were synthesized *via in situ* reductions by exploiting the inherent reducibility of MoS_2 (Fig. 9).[114] The differential binding interactions of different biomolecules and metal NPs induced peroxidase-like property modulation of metal NP-decorated PPy@MoS_2. On the basis of this, a cross-reactive colorimetric sensor array-based PPy@MoS_2@Au/Ag/Pd was developed for the accurate and effective discrimination of 11 proteins and 5 oral bacteria with substrates of TMB and H_2O_2.

In addition, other metal sulfide-based nanozymes, such as vanadium disulfide (VS_2), copper sulfide (CuS), and platinum disulfide (PtS_2), with specific morphologies also possess intrinsic peroxidase-like behavior. They were chosen as a useful and dependable colorimetric probe for the determination of H_2O_2 and glucose in real samples. For instance, Huang LJ and co-workers combined VS_2 nanozymes and GOx to design a colorimetric cascade assay for the detection of glucose by employing the catalyzed TMB-H_2O_2 reaction.[115] In brief, GOx was first

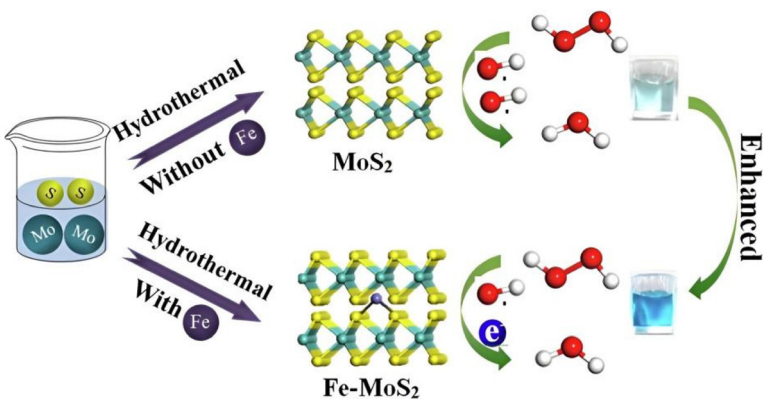

Fig. 8 Schematic diagram of enzyme activity comparison of MoS_2 and Fe-MoS_2 prepared using a hydrothermal method.[112]

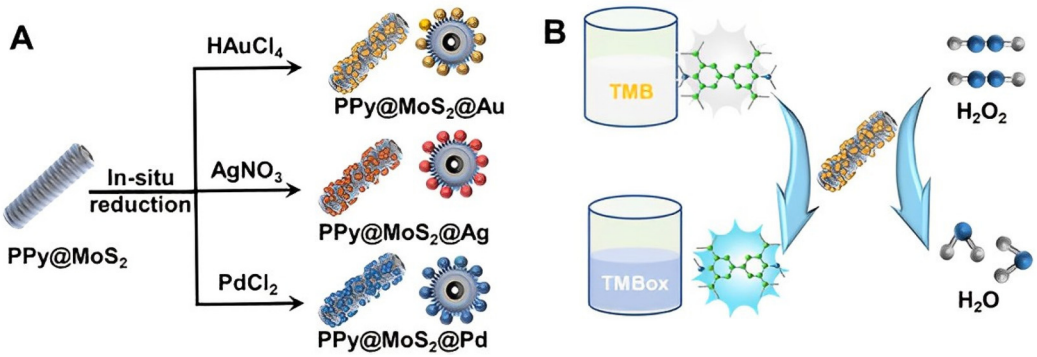

Fig. 9 (A) Schematic illustration of Au, Ag, and Pd NP-decorated PPy@MoS_2 nanocomposites prepared by *in situ* reduction and (B) PPy@MoS_2@Au catalytic oxidation of TMB.[114]

incubated with glucose for catalytic oxidation to generate gluconic acid and H_2O_2 with the existence of O_2. After that, the reaction between VS_2 and TMB was initiated using the resultant H_2O_2, causing a blue color solution. Ultimately, the glucose concentration was indirectly detected using the resulting color as colorimetric signals. As with this colorimetric assay principle, Swaidan A. *et al.*[116] and Zhang W. X. *et al.*[117] integrated CuS/PtS_2-based nanozymes with GOx to demonstrate a colorimetric cascade method for sensing H_2O_2 and glucose.

4.2 Metal selenide-based nanozymes

Molybdenum diselenide ($MoSe_2$) possesses intrinsic peroxidase mimetic activity, which has emerged as a promising candidate in various colorimetric assays. Wu XJ and coworkers first pointed out that few-layer $MoSe_2$ nanosheets displayed great potential as peroxidase mimics.[118] Firstly, xanthine produced H_2O_2 and uric acid under the action of xanthine oxidase. Then, using a liquid exfoliation method, few-layer $MoSe_2$ nanosheets were obtained for catalyzing the oxidation of TMB-H_2O_2 to a blue oxidative product in aqueous media. Based on this catalytic mechanism, a highly sensitive and selective colorimetric approach was developed for the determination of H_2O_2 and xanthine.

Moreover, the large surface area of $MoSe_2$ nanosheets was compatible with different surface engineering tactics. Chitosan was conjugated onto $MoSe_2$ nanosheets (CS-$MoSe_2$ nanosheets) surface through a one-step ionic liquid-assisted grinding approach for the colorimetric determination of Hg^{2+}.[119] When Hg^{2+} was introduced, chitosan molecules captured Hg^{2+}, and partial Hg^{2+} was *in situ* reduced to Hg^0 on the surface of CS-$MoSe_2$ nanosheets. Hence, the peroxidase-like properties of CS-$MoSe_2$ nanosheets were enhanced by the activating effect of Hg^{2+}. Using TMB as a chromogenic dye, a sensitive and rapid platform for the colorimetric detection of Hg^{2+} was established by integrated low cytotoxicity CS-$MoSe_2$ nanosheets sensor and a smartphone detection device, with a lower LOD of 8.4 nM (Fig. 10). Lin L. and coworkers recently synthesized $MoSe_2$@Fe-based nanozymes *via* a one-pot hydrothermal strategy for the colorimetric sensing of Fe^{3+} and GSH.[120] $MoSe_2$@Fe with peroxidase mimetic property catalyzed the oxidation of TMB-H_2O_2 to form blue oxTMB solution. The enzymatic activity increased (or decreased) when Fe^{3+} (or GSH) was added, resulting in a deepening (or weakening) of the blue color of the system, allowing quantitative and selective recognition of Fe^{3+} and GSH in food samples.

5. Carbon-based nanozymes

In 2010, Song Y. J. *et al.* showed that single-walled carbon nanotubes (SWCNTs) possessed intrinsic peroxidase-mimicking performance, catalyzing the reaction of substrate TMB-H_2O_2 to generate a blue color.[121] Due to fascinating enzyme mimetic activity, low toxicity, high stability, and good biocompatibility, carbon-based nanomaterials, such as graphene oxides (GO), graphitic carbon nitride (g-C_3N_4), single atom nanozymes (SAzymes) and carbon dots have aroused growing interest in nanozyme-based colorimetric assays.

5.1 GO-based nanozymes

GO is a 2D material with a honeycomb lattice composed of sp^2 carbon atoms, which has a large specific surface area, high electron mobility, and mechanical strength. Qu's and Ren's groups reported that carboxy-modified GO (GO-COOH) possessed intrinsic peroxidase-like activity that catalyzed the oxidation of the TMB-H_2O_2 system to produce a blue color signal.[122] Based on their findings, they established a glucose colorimetry assay using the catalytic activity of GOx and GO-COOH peroxidase (Fig. 11). Subsequently, the same group first synthesized GO-Au NCs hybrid (GA) by simply absorbing Au NCs on GO through the electrostatic interactions, which exhibited excellent peroxidase-like activity.[123] Using folic acid conjugated GO-Au NCs hybrid, they designed a simple, low-cost, highly selective and sensitive colorimetric sensor for the detection of cancer cells.

However, the dispersion of metals and metal oxide NPs on GO nanosheets in a unique 2D layer assembly hinders their aggregation induction, leading to a decrease in enzyme-like activity. To solve this limitation, Sun H. Y. *et al.* prepared

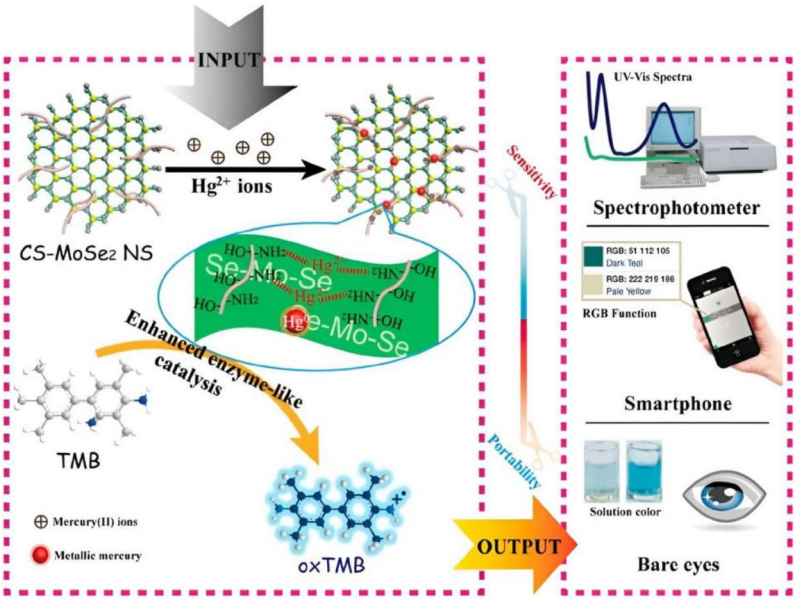

Fig. 10 Versatile colorimetric detection diagram of Hg^{2+} based on CS-$MoSe_2$ nanosheets.[119]

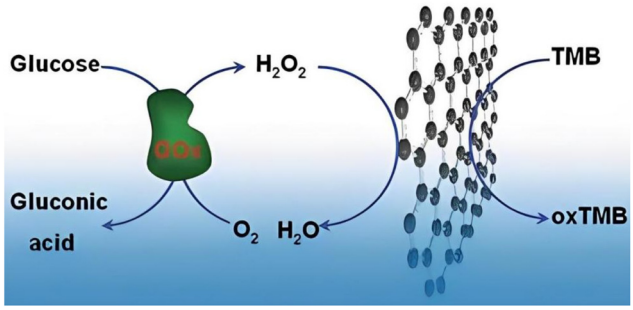

Fig. 11 Schematic diagram of a colorimetric approach for the detection of glucose based on GOx and the GO-COOH catalyzed TMB-H_2O_2 system.[122]

small-sized iridium oxide (IrO_2) NPs supported on polyallylamine (PAH)-modified GO nanosheets *via* electrostatic interactions by employing a facile and environment-friendly pulsed laser ablation in liquid (PLAL) method.[124] Due to the large surface area and anchor sites, the choice of GO modified with PAH as the carrier of IrO_2 was beneficial to reduce the aggregation of GO while extending the reaction time. The high peroxidase-like activity of the IrO_2@GO nanozymes was derived from accelerated electron transfer rather than dependent on $^{\bullet}OH$ production. Upon the introduction of AA, the admirable peroxidase-mimicking properties of IrO_2@GO nanozymes could be inhibited. Herein, a colorimetric probe based on the IrO_2@GO-H_2O_2-TMB reaction system was constructed for sensing AA.

Additionally, using PEG derivatives as coupling linkers, Zhang S. T. and coworkers first synthesized strongly coupled Au/Fe_3O_4/GO hybrid materials.[125] Owing to the abundant functional groups with remarkable hydrophilicity and high surface area in GO, the aggregation of Au and Fe_3O_4 NPs was reduced while the deposition of Hg^0 on the Au surface was increased. Moreover, the use of superparamagnetic Fe_3O_4 as a carrier can facilitate the recovery of ternary hybrid materials. The authors further demonstrated that Hg^{2+} could stimulate the peroxidase-like property of Au/Fe_3O_4/GO hybrid materials for ultrasensitive colorimetric sensing of Hg^{2+} by catalyzing TMB with H_2O_2. Furthermore, Adegoke O. *et al.* successfully anchored Au NPs and CeO_2 NPs onto GO nanosheet surfaces using a chemically modified means.[126] In the presence of nitrite, nitrite drove the redox cycle of Au NP-CeO_2 NP@GO nanozymes to rapidly catalyze the oxidation of colorless TMB to produce a unique green color signal without H_2O_2 (Fig. 12). Therefore, a colorimetric sensor based on AuNP-CeO_2 NP@GO nanozymes was developed for the colorimetric determination of nitrite in tap water.

Compared with bimetallic NPs catalysts, bimetallic oxide NPs nanozymes are rarely investigated. Accordingly, Das's group reported low-cost Fe_3O_4–TiO_2 decorated on the reduced GO (rGO) nanosheets through a simple hydrothermal method.[127] rGO nanosheets could promote the interaction of composites with targeted molecules *via* π–π interactions. Benefiting from the synergistic effects of Fe_3O_4 NPs and TiO_2 NPs, magnetic Fe_3O_4–TiO_2/rGO-based nanozymes improved the activity of peroxidase-like catalysis for the colorimetric detection of atrazine pesticide by oxidizing TMB-H_2O_2 (Fig. 13). Similarly, a novel nanozyme for the modification of Fe_3O_4 NPs, CuO NPs, and cucurbit[6]uril (CB[6]) onto the surface of GO was fabricated by employing a facile sonochemical technique.[128] In Fe_3O_4-CuO-CB[6]-GO nanozymes, CB[6] as a specific binding pocket equipped nanozymes with molecular recognition ability, and the synergistic effect of Fe_3O_4-CuO-GO

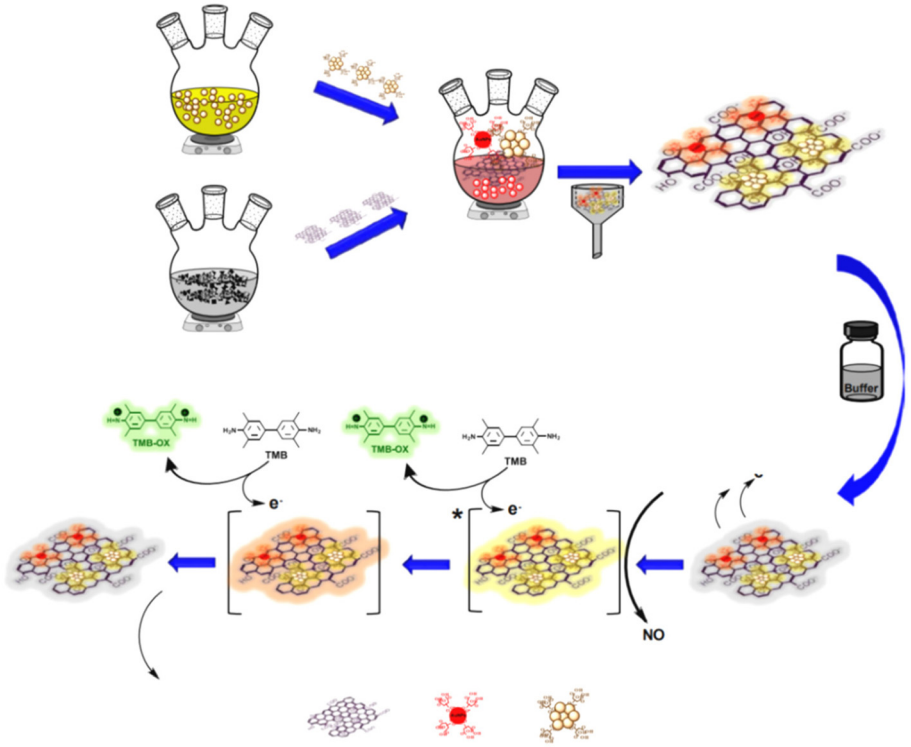

Fig. 12 Schematic illustration of the synthesis of Au NP-CeO_2 NP@GO nanozymes and their use for colorimetric detection of nitrite.[126]

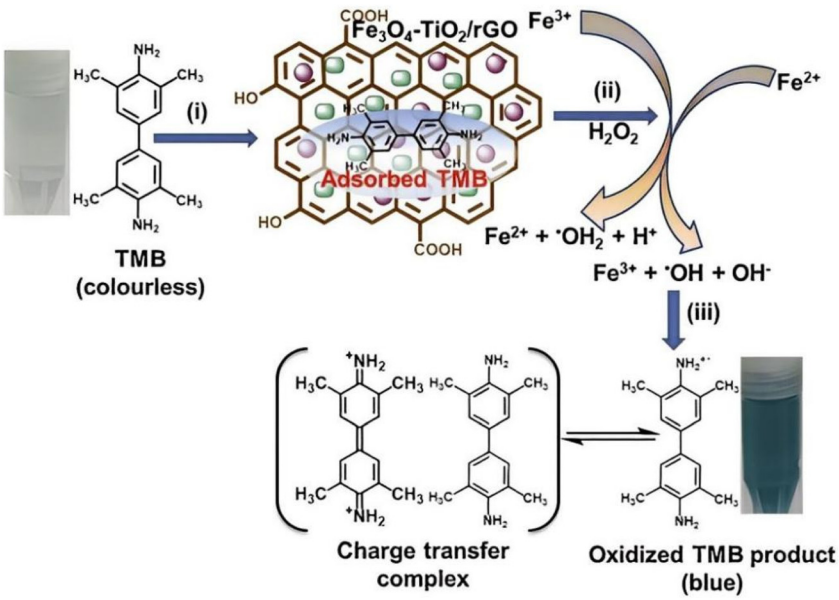

Fig. 13 Schematic illustration of (i) TMB adsorbed on the surface of Fe_3O_4–TiO_2/rGO nanozymes, (ii) ·OH generated by the Fenton reaction, and (iii) TMB oxidized by ·OH radicals.[127]

facilitated the improvement of the peroxidase-mimicking activity. Attributable to the inhibition effect of homocysteine (Hcy) towards the oxidation of TMB-H_2O_2 catalyzed by Fe_3O_4-CuO-CB[6]-GO nanozymes, a sensitive and selective colorimetric approach was thereby established for the detection of Hcy, with a LOD of 1.8 μM. In addition, other GO-based nanozymes, such as Prussian blue (PB),[129] cetyltrimethylammonium bromide (CTAB),[130] ganoderma polysaccharide (GP),[131] and quantum dot (QD)[132] incorporated GO also possessed the excellent properties of simulating peroxidase with

higher catalytic activity. Accordingly, the ultrasensitive colorimetric biosensor was established for the detection of apolipoprotein A1 (ApoA1), amphetamine (AMP), methamphetamine (MAMP), L-cysteine (L-Cys) and H_2O_2, respectively.

5.2 g-C_3N_4-based nanozymes

g-C_3N_4, as a typical metal-free semiconductor, possesses a 2D graphene-layered structure, which exhibits enzyme-like activity due to its unique structure and property. However, compared with GO, the activity of g-C_3N_4 nanosheets appears very weak. Therefore, some metal ions or metal oxides were used to dope or modify g-C_3N_4 for remarkably enhancing the catalytic performance of g-C_3N_4. For example, Zhao X. T. *et al.* prepared spherical g-C_3N_4/CeO_2 nanozymes by *in situ* growth of CeO_2 NPs on g-C_3N_4 nanosheets.[133] The synergistic introduction of g-C_3N_4 nanosheets facilitated the electron transfer of CeO_2, which significantly improved the catalytic activities of g-C_3N_4/CeO_2 nanozymes, and catalyzed the oxidation of TMB to give a blue signal. Surprisingly, due to the strong interaction between Hg^{2+} and the nitrogen of g-C_3N_4, g-C_3N_4/CeO_2 nanozymes would be aggregated, resulting in a reasonable reduction of catalytic capacity in the presence of Hg^{2+}. As a result, a selective and sensitive colorimetric platform based on g-C_3N_4/CeO_2 nanozymes was developed for sensing Hg^{2+} in blood and wastewater samples containing complex matrices. Shen Y. Z. *et al.* introduced Cu^{2+} into g-C_3N_4 to fabricate Cu-doped-g-C_3N_4 nanocomposite-based nanozymes for evaluating residual antibiotics in food and agriculture-related matrices.[134] Due to the synergistic coordination arising from abundant Cu^{2+} and g-C_3N_4 nanosheets, Cu-doped-g-C_3N_4 nanocomposite-based nanozymes exhibited impressive peroxidase-mimicking activity. As expected, it displayed a high affinity for catalyzing colorless TMB-H_2O_2 to generate a steel-blue oxTMB product. Upon the introduction of tetracycline (TC), the effect of Cu-doped-g-C_3N_4 nanozymes on the catalytic substrates was significantly blocked, which was due to the blocking effect of the π–π stacking interaction between the TC tetraphenyl skeleton and nanozymes. As a result, the residual concentration of TC increased, and the visual color could be observed from steel-blue to light-blue. Based on this principle, a smartphone-based colorimetric assay was built to perform the quantitative analysis of TC in milk, with a LOD of 86.27 nM.

Moreover, g-C_3N_4 nanozymes have been shown to absorb single-stranded DNA (ssDNA). The high affinity between g-C_3N_4 and ssDNA enables g-C_3N_4/ssDNA sensing platforms to specifically recognize target molecules. However, the catalytic activity of g-C_3N_4 nanosheets against H_2O_2 is low. To break through this bottleneck, Fan Y. F. *et al.* prepared a novel nanozyme based on 3D branched carbon nitride nanoneedles (3DBC-C_3N_4).[135] The 3D branched structures possessed a large specific surface area and plenty of active sites, which promoted electron transfer and induced a lightning-rod-like effect to accelerate the electron collection in the tip region for activating H_2O_2 (Fig. 14). Therefore, 3DBC-C_3N_4 nanozymes can adsorb more target molecules for the catalytic reaction and improve catalytic activity. With the activation of H_2O_2 to the formation

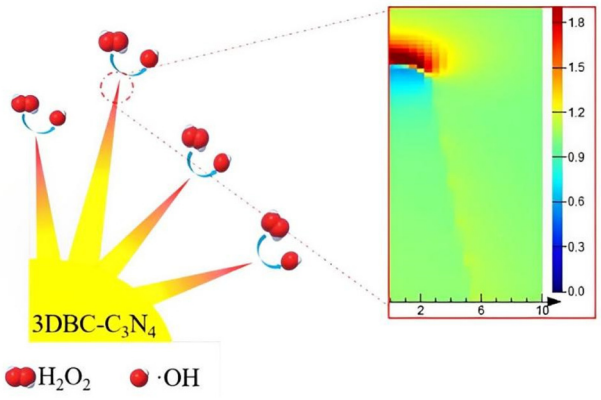

Fig. 14 Schematic diagram of the 3DBC-C_3N_4 nanozymes accelerating electron collection in the tip region to activate H_2O_2 to produce $^{\bullet}OH$.[135]

of $^{\bullet}OH$, 3DBC-C_3N_4 with excellent peroxidase-like activity catalyzed the oxidation of TMB in the presence of H_2O_2. In addition, ssDNA accelerated the oxygenation of TMB through electrostatic interaction, thus improving the peroxidase-like activity of 3DBC-C_3N_4 nanozymes. The increased concentration and length of ssDNA further enhanced the catalytic oxidation of TMB by 3DBC-C_3N_4 nanozymes, which could also be employed for the colorimetric detection of oxytetracycline (OTC).

5.3 Single-atom nanozymes

Traditional nanozymes generally face enormous challenges of low activity and poor specificity ascribed to their different crystalline nanostructures and diverse surface configurations. Toward this end, single-atom nanozymes (SAzymes) with isolated metal atoms anchored on nitrogen-enriched carbon material supports have attracted extensive attention in catalysis and biosensing fields. SAzymes with uniformly dispersed active sites hold nearly 100% atom utilization efficiency and maximum specificity, which are reckoned as ideal nanozymes with favorable catalytic activity and selectivity.[136,137]

Zhou X. B. *et al.* prepared Fe–N–C SAzymes showing exceedingly good peroxidase-mimicking activity and specificity *via* an isolation-pyrolysis approach.[138] While galactose oxidase (Gal Ox) catalyzed the oxidation of galactose to generate H_2O_2, Fe–N–C SAzymes further catalyzed the oxidation of TMB-H_2O_2 to produce a blue signal. Such an enzymatic cascade reaction based on Gal Ox and Fe–N–C SAzymes realized the rapid and sensitive quantitative colorimetric detection of galactose. Similarly, Mao Y. and coworkers reported a novel colorimetric assay for the determination of Cr(VI) ions using Fe–N–C SAzymes.[139] Using 8-hydroxyquinoline (8-HQ) as an inhibitor could prevent Fe–N–C SAzymes from catalyzing the oxidation of TMB to generate blue oxTMB products. When Cr(VI) ions were added, due to their strong chelating capability, the preferential binding of Cr(VI) ions to 8-HQ ultimately led to blue color recovery. According to this phenomenon, an ultrahigh sensitive and selective colorimetric platform based on Fe–N–C

SAzymes was proposed for sensing Cr(VI) ions, with a lower LOD of 3 nM. However, many SAzymes have the disadvantages of low dispersion of aqueous solution and lack of recognition ability, which hinders their application in biological analysis. Therefore, Sun L. P. *et al.* synthesized DNA/Fe–N–C SAzymes conjugates by engineering DNA modification to Fe–N–C SAzymes.[140] This significantly enhanced the dispersibility of Fe–N–C SAzymes without affecting the peroxidase-like activity of Fe–N–C SAzymes. A HePG2 cancer cell sensor was established based on a diblock DNA (one polyadenine and one aptamer DNA sequence) attached to Fe–N–C SAzymes in HEPES containing $MgCl_2$ (Fig. 15A). Apt/Fe–N–C SAzymes, after binding to HePG2 cancer cells with aptamer-targeting receptors, catalyzed the oxidation of the TMB-H_2O_2 system to produce the blue signal (Fig. 15B).

In recent years, sensors based on nanozymes with enzyme-like activity have been employed for the rapid and low-cost detection of antioxidants. However, most colorimetric sensors based on nanozymes are single sensors that can only detect one type of antioxidant, and also have very limited specificity. Herein, a colorimetric sensor array based on SAzymes was designed to recognize a variety of biological antioxidants. For instance, Jing W. J. *et al.* constructed a three-channel colorimetric sensor array based on Fe–N–C SAzymes for the simultaneous discrimination of five representative biological antioxidants including GSH, L-Cys, AA, uric acid (UA), and melatonin (MT).[141] Fe–N–C SAzymes could catalyze the oxidation of TMB, OPD, and ABTS, respectively, generating blue oxTMB, yellow oxOPD, and green oxABTS. When different contents of GSH, L-Cys, AA, UA, and MT were added, the sensing probes of oxTMB, oxOPD, and oxABTS were reduced to diverse degrees, respectively, also being accompanied by different color responses. Thus, a three-channel colorimetric sensor array was fabricated to accurately identify five representatives as low as 100 nM in human serum samples through the linear discriminant analysis (LDA). Following the same detection principle, Liu B. and coworkers developed a Co–N–C SAzymes-based array sensor with a simpler design and more sensitive detection for distinguishing seven antioxidants: GSH, AA, Cys, tannin (TA), catechin (C), DA and UA, with the lowest LODs of 10 nM (Fig. 16).[142] The identification and quantitative analysis of multiple target antioxidants were achieved using the colorimetric changes as fingerprints attributed to the different catalytic abilities of Co–N–C SAzymes at pH 3.6 and 4.8 as array receptors.

5.4 Other carbon-based nanozymes

As a carbon nanostructure with a size of less than 10 nm, carbon dots that mimic the structure and function of natural enzymes have the advantages of easy modification, low toxicity, and good biocompatibility. Recently, C-dots/Mn_3O_4 nanocomposites were synthesized chemically and further verified with various techniques.[143] Compared with Mn_3O_4 NPs, C-dots/Mn_3O_4 nanocomposites showed higher intrinsic oxidase-like activity. In the presence of O_2, C-dots/Mn_3O_4 nanozymes catalyzed the oxidation of TMB to produce a blue color solution. Once ferrous ions (Fe^{2+}) were introduced, the blue color faded to varying degrees due to the competition reaction between Fe^{2+} and TMB. In this way, a highly sensitive and selective colorimetric sensor based on a cheap C-dot/Mn_3O_4 nanozyme probe was established for sensing Fe^{2+}, with a LOD of 0.03 μM.

Additionally, enzymatic cascade reactions of other carbon-based nanozymes, such as carbon support material, carbon quantum dot (CQD), and graphdiyne oxide (GDYO), with natural enzymes have also been employed in colorimetric detection investigations. Ren H. *et al.* first synthesized MoO_3 nanorod-supported carbon materials (MoO_3/C) with outstanding peroxidase-mimicking activity utilizing a green tide biomass template (Fig. 17).[144] As-synthesized MoO_3/C combined with the GOx cascade reaction were applied for constructing colorimetric sensors for the sensitive detection of

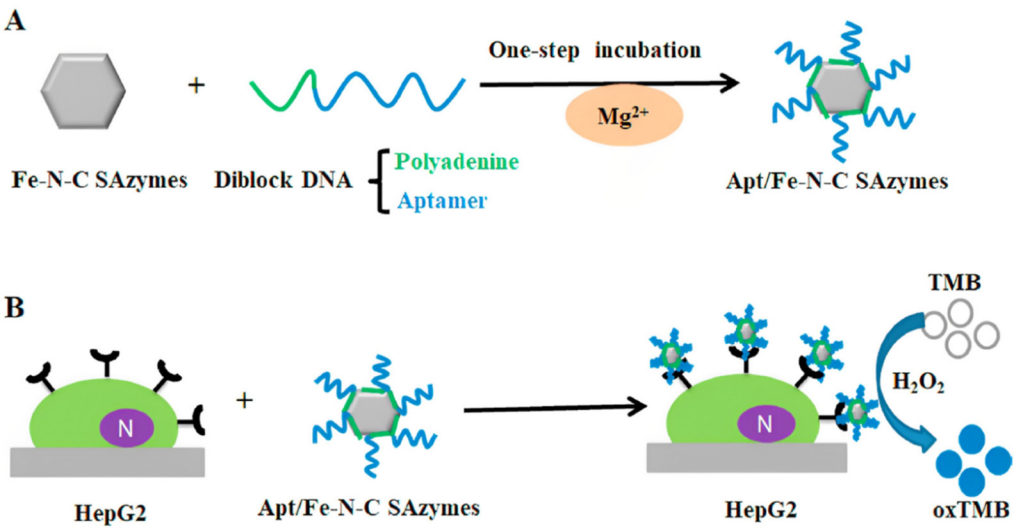

Fig. 15 Schematic diagram of Apt/Fe–N–C SAzymes preparation (A) and colorimetric detection of HePG2 cancer cells (B).[140]

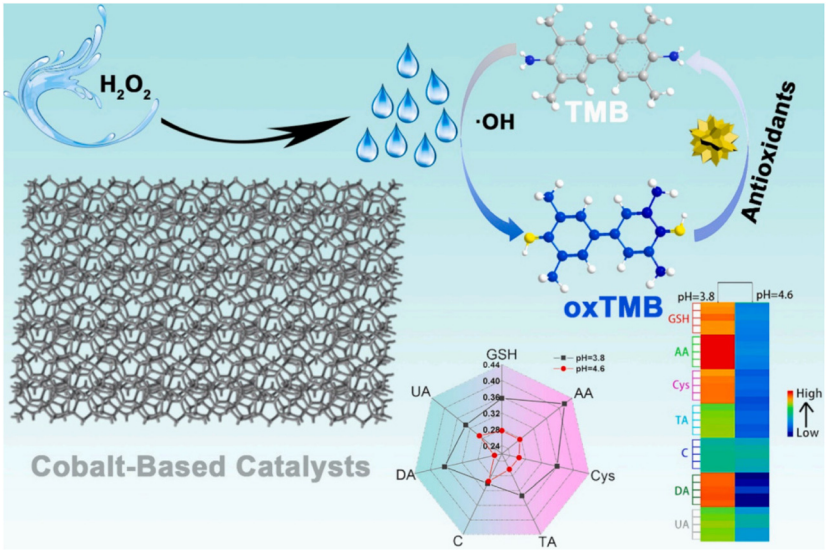

Fig. 16 Schematic diagram of identifying seven antioxidants based on the sensor array of Co–N–C SAzymes as sensor units at different pH values.[142]

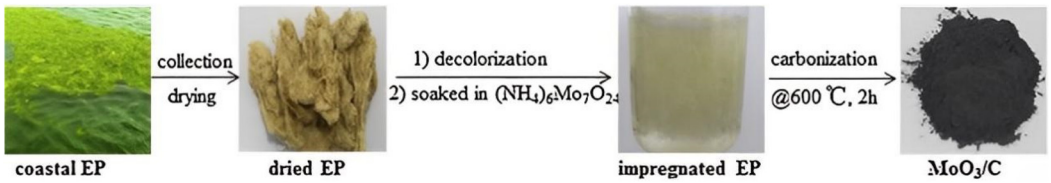

Fig. 17 Preparation of MoO_3/C nanorods by a green tide biomass template.[144]

glucose by using TMB as chromogenic substrates. The process of applying MoO_3/C nanozymes to detect glucose mainly consisted of two steps. Under the catalysis of GOx, glucose was initially oxidized by O_2 to gluconic acid and H_2O_2, and then the synthesized H_2O_2 further oxidized TMB, inducing a color change in the presence of MoO_3/C nanozymes. By the same principle, as described above, Mo, S-co-doped CQD (Mo-CQDs), and hemin/GDYO nanocomposites formed cascade reactions with ChOx and GOx, respectively, for colorimetrically sensing cholesterol[145] and glucose.[146] These studies have greatly broadened the application range of carbon-based nanozymes.

6. Metal–organic frameworks-based nanozymes

Metal–organic frameworks (MOFs) are self-assembled from common metal ions and organic cross-linking agents. Due to their unique porous structures and large specific surface areas, MOFs have been considered as flourishing research materials for the construction of nanozymes. The ordered arrangement of metal nodes and organic ligands provides MOFs with abundant accessible catalytic sites and endows MOFs with inherent enzyme-like activities for applications in colorimetric assays. The applications of MOFs in nanozymes mainly include the peroxidase-like activity of MOFs themselves and the use of MOFs as carriers for various enzymes. It is worth noting that one of the effective ways to further improve the catalytic performance is to modulate the composition of MOF-based nanozymes by metal doping (such as Fe, Ni, Co, and Mn).

At present, Fe-doped MOFs with peroxidase-like activity have been demonstrated for the colorimetric detection of biomolecules. For example, Chen N. *et al.* developed a naked-eye and point-of-care testing sensor based on Fe-MOFs nanozymes for immunoassay colorimetric determination of *Salmonella* enteritidis (*S.* enteritidis).[147] The basic principle of colorimetric determination was as follows. Ab1 (mouse anti-Salmonella monoclonal antibody) modified nanozymes will combine with Ab2-modified magnetic beads (Dynabeads™ anti-Salmonella) through a specific interaction between Ab1, Ab2, and *S.* enteritidis with the addition of target virus. In this manner, the formed sandwich structure "Ab1-modified nanozymes-*S.* enteritidis-Ab2 modified magnetic beads" were removed from the supernatant with an external magnet. After magnetic separation, residual Fe-MOFs nanozymes that were not bound to the target could not be removed due to the lack of the attached magnetic beads. Therefore, using TMB-H_2O_2 as

colorimetric substrates, *S.* enteritidis can be measured indirectly and successfully by residual Fe-MOFs nanozymes promoting the oxidation of TMB to generate different degrees of blue color signals in the supernatant. Since the Fe-doped MOFs nanozymes enhanced the sensing signal, *S.* enteritidis can be detected with a lower LOD of 34 CFU mL^{-1}. Furthermore, MIL-53(Fe) was chosen as MOFs-based nanozymes, serving to realize the colorimetric detection of salicylic acid (SA) in aspirin.[148] MIL-53(Fe) prepared using a solvothermal method exhibited favorable peroxidase-mimicking activity, which catalyzed the oxidation of TMB in the presence of H_2O_2 and rendered it blue. Notably, the catalytic activity of MIL-53(Fe) was clearly suppressed after the introduction of SA, which displayed a lighter blue color due to the complexation reaction of SA with Fe^{3+} at the center of MIL-53(Fe) (Fig. 18). Accordingly, a high selectivity and sensitivity approach based on MIL-53(Fe) MOF nanozymes was proposed for the sensing of SA, with a LOD of 0.26 μM.

In recent years, Cu-MOF nanozymes systems have not been effectively applied due to the mutual interference between the properties of various enzymes. To address this issue, Ying M. H. and coworkers explored a novel Cu/fumaric acid (FMA)-MOFs with high bifunctional nanozyme activities and good anti-interference properties.[149] Cu^{2+} and Cu^{+} active centers existed on the surface of Cu/FMA, which showed peroxidase and laccase-like activities under pH = 4 and 8, respectively. Accordingly, a dual-mode colorimetric platform based on Cu/FMA-MOFs was established for detecting glucose and epinephrine in human serum.

Relative to that of the single-metal MOFs, the bimetallic MOFs formed by the partial replacement of the original metal nodes with other metal ions possess higher nanozymes catalytic activity. In principle, doping two metal elements in the initial MOFs can enhance the catalytic activity due to the good synergistic electron transfer effects between various metals. For instance, 2D Ni/Fe-MOFs nanosheets were prepared using a simple two-step sonication method at room temperature.[150] With strong intrinsic peroxidase-like activity, 2D Ni/Fe MOFs nanosheets could catalyze the oxidation of the TMB-H_2O_2 reaction system from colorless to blue. The addition of glutathione could markedly inhibit the peroxidase-like activity of 2D Ni/Fe-MOF nanosheets. Interestingly, due to the high specific affinity of Hg^{2+} for thiol groups in glutathione, further introduced Hg^{2+} could restore the suppressed TMB oxidation. According to the above principles, a colorimetric platform based on 2D Ni/Fe-MOFs nanosheets was constructed to recognize multiple targets, including H_2O_2, glutathione, and Hg^{2+}, with LODs of 10 nM, 10 nM, and 100 nM, respectively. Due to the high density of active metal sites in 2D Ni/Fe-MOFs nanosheets, the synergistic effect between Ni and Fe strengthened the intrinsic catalytic behavior of each site. Meanwhile, as demonstrated from the UV-Vis spectra, compared with single-metal Ni-MOFs and Fe-MOFs, the peroxidase-like activities of the 2D Ni/Fe-MOFs nanosheets were enhanced by over 14-fold and 3-fold, respectively.

Subsequently, Zhao X. L. *et al.* designed a simple, rapid, and cost-effective colorimetric approach based on Co/Fe-MOFs-iodide (I^-) nanozymes for detecting hydrogen sulfide (H_2S) in real serum samples.[151] In the presence of H_2O_2, Co/Fe-MOFs and I^- could synergistically catalyze TMB to blue oxTMB, thereby enhancing the catalytic performance of Co/Fe-MOFs-I^-. When H_2S was present, the color rendering effect of TMB was suppressed and the system appeared a lighter blue (Fig. 19). A novel ultrahigh sensitivity H_2S colorimetric platform was therefore established, with the lowest LOD of 0.33 nM. While in the absence of I^-, the LOD was approximately 200 times higher than that from the amplified colorimetric assays.

The synthesis conditions of most MOFs (*i.e.* Fe-MOF and Cu-MOF) are harsh, generally requiring high temperature and high pressure, as well as numerous organic reagents. Nonetheless, biomimetic zeolitic imidazolate frameworks (ZIF)

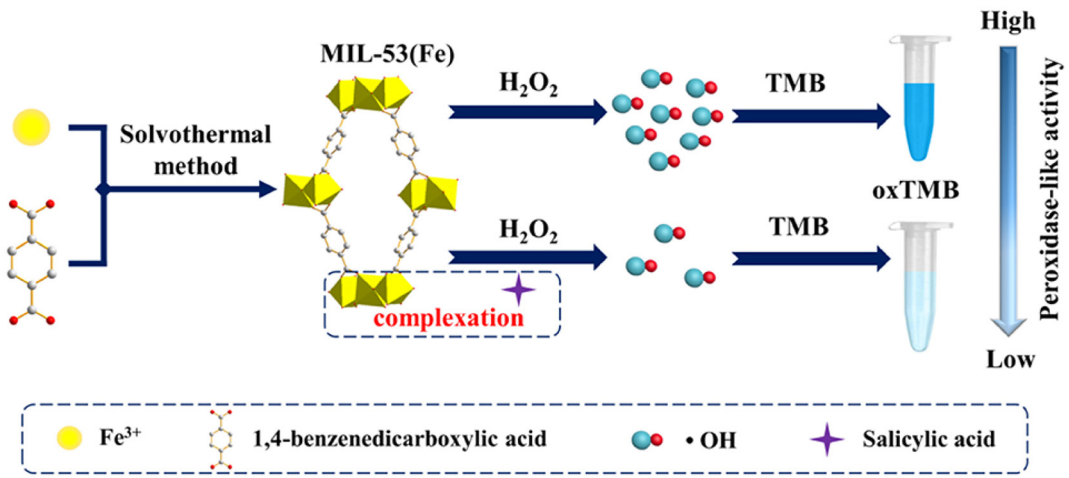

Fig. 18 Schematic diagram of MIL-53(Fe) synthesized using the solvothermal method and the colorimetric detection of SA based on MIL-53(Fe) MOFs nanozymes.[148]

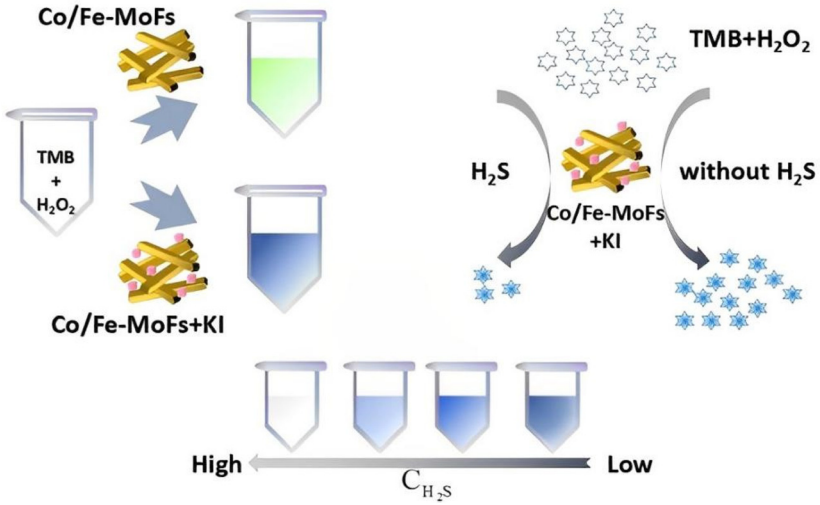

Fig. 19 Schematic illustration of H_2S detection by Co/Fe-MOFs-I^- nanozyme-based colorimetric sensors.[151]

have attracted extensive attention due to their promising biocompatibility, diverse enzyme-like activities, and facile synthetic conditions. Nataraj N. *et al.* reported a novel Co-ZIF-67 nanozyme *via* a simple co-precipitation method at room temperature.[152] Co-ZIF-67 nanozymes exhibited intrinsic peroxidase-mimicking performance and effectively oxidized TMB to produce blue oxTMB in the presence of H_2O_2. Interestingly, the abundant availability of Co-ZIF-67 active sites binding acetaminophen provided enhanced catalytic properties. Different concentrations of acetaminophen could oxidize TMB to generate varying degrees of dark blue. As a result, Co-ZIF-67 nanozymes were employed for the colorimetric detection of acetaminophen. Furthermore, Ran F. P. *et al.* first constructed a novel nanozyme sensor by utilizing the self-assembly of Au NCs and ZIF-8/polyamine functionalized quantum dots (CQDs).[153] They found that the peroxidase-like activity of Au NCs can be significantly enhanced by heparin in the physiological environment (pH 7.4). Accordingly, the catalytic activity of Au NCs-ZIF-8/CQD nanozmes on TMB-H_2O_2 substrate was significantly improved (Fig. 20). Once protamine was introduced, due to the specific binding of protamin to heparin, heparin was unable to adsorb on the surface of ZIF-8/CQDs, thus significantly inhibiting the enhancement of the catalytic activity of Au-NCs. Based on the above facts, a facile and efficient colorimetric method was proposed for the quantitative detection of heparin and protamine in biological samples. These studies provide valuable references for designing MOFs-based nanozymes in colorimetric assays.

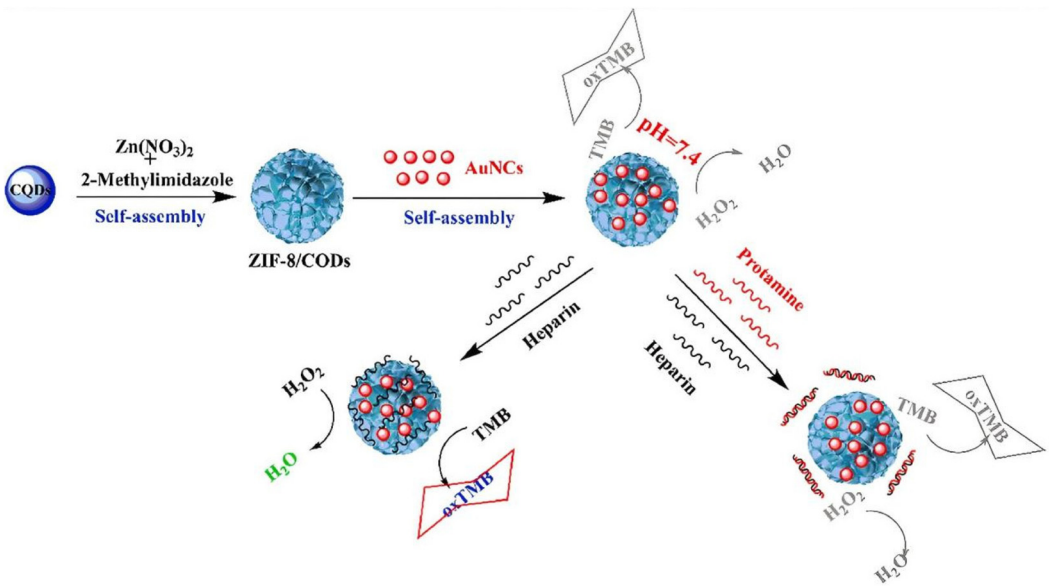

Fig. 20 Schematic illustration of the colorimetric determination of heparin and protamine.[153]

7. Conclusion and prospects

This review outlines the research progress and applications of colorimetric sensors based on nanozymes with peroxidase-like activity in diverse fields over the past decade. Due to the advantages of nanozymes with more flexible structure, high stability, and ease of modification, nanozyme-based colorimetric sensors have emerged as promising alternative tools for the rapid, simple, and low-cost detection of analytes. Although remarkable progress has already been made in colorimetric sensors based on nanozymes with peroxidase-like activity, several challenges and obstacles remain in this frontier field.

(1) Since nanomaterials are easily aggregated and unstable, how to improve the catalytic activity and stability of nanozymes has become an urgent problem to be solved. Hence, modifying the surface of nanomaterials to synthesize efficient nanozymes with high catalytic activity and high affinity will be the focus of future research.

(2) In the detection of real biological samples, the non-specific adsorption of proteins to nanozymes will affect the catalytic activity of nanozymes, resulting in unsatisfactory detection results. For the development of novel nanozymes with high utilization, it is necessary to further investigate the anti-interference of their enzyme-like activities.

(3) In recent years, the potential safety, environmental, and health concerns of nanozymes have drawn public and academic attention to their toxicity. Faced with this challenge, besides the nanomaterials themselves, surface coatings and modifications should also be considered.

(4) In addition, considering the diversity of natural enzymes, designing nanozymes with novel catalytic properties, such as hydrolases and synthases, to greatly improve the selectivity of nanozymes will also be the focus of future work.

To sum up, although nanozyme-based colorimetric biosensors show broad prospects, the practical applications of basic and leading scientific achievements in clinical diagnosis, food analysis, immunoassay, and environmental monitoring requires more effort. We hope that this review can provide a certain reference value for the synthesis of nanozymes and their application in colorimetric analysis, which is helpful for their future development.

Author contributions

Chi Zhongmei: Conceptualization, methodology, validation, investigation, resources, supervision, writing-original draft, writing-review & editing. Wang Qiong: Supervision. Gu Jiali: Conceptualization.

Conflicts of interest

The authors declare no competing financial interest.

Acknowledgements

The authors gratefully acknowledge the financial support from the Initializing Foundation of Doctors in Bohai University (Grant No. 05013-0521bs018), Bohai University School-Level Scientific Research Project (Grant No. 05015-0522xn043), and the Doctoral Scientific Research Foundation of Liaoning Province (Grant No. 2023-BS-801).

References

1 N. Ullah, M. Mansha, I. Khan and A. Qurashi, *TrAC, Trends Anal. Chem.*, 2018, **100**, 155–166.
2 A. Azzouz, S. K. Kailasa, P. Kumar, E. Ballesteros and K. H. Kim, *TrAC, Trends Anal. Chem.*, 2019, **113**, 256–279.
3 M. A. Al Mamun and M. R. Yuce, *Adv. Funct. Mater.*, 2020, **30**, 2005703.
4 L. Z. Gao, J. Zhuang, L. Nie, J. B. Zhang, Y. Zhang, N. Gu, T. H. Wang, J. Feng, D. L. Yang, S. Perrett and X. Y. Yan, *Nat. Nanotechnol.*, 2007, **2**, 577–583.
5 H. Wei and E. K. Wang, *Chem. Soc. Rev.*, 2013, **42**, 6060–6093.
6 Q. Q. Wang, H. Wei, Z. Q. Zhang, E. K. Wang and S. J. Dong, *TrAC, Trends Anal. Chem.*, 2018, **105**, 218–224.
7 J. J. X. Wu, X. Y. Wang, Q. Wang, Z. P. Lou, S. R. Li, Y. Y. Zhu, L. Qin and H. Wei, *Chem. Soc. Rev.*, 2019, **48**, 1004–1076.
8 Y. Y. Tian, Y. C. Chen, M. Chen, Z. L. Song, B. Xiong and X. B. Zhang, *Talanta*, 2021, **221**, 121627.
9 B. Zhang, Y. J. Lv, C. G. Yu, W. Zhang, S. S. Song, Y. X. Li, Y. Chong, J. Huang and Z. J. Zhang, *Biomater. Adv.*, 2022, **137**, 212869.
10 Z. Zhou, Y. L. Wang, F. Peng, F. Q. Meng, J. J. Zha, L. Ma, Y. H. Du, N. Peng, L. F. Ma, Q. H. Zhang, L. Gu, W. Y. Yin, Z. J. Gu and C. L. Tan, *Angew. Chem., Int. Ed.*, 2022, **61**, e202115939.
11 J. Q. Zha, W. G. Wu, P. Xie, H. H. Han, Z. Fang, Y. T. Chen and Z. F. Jia, *Catalysts*, 2022, **12**, 614.
12 S. Zhang, P. Li, S. Chu, L. P. Feng, S. Li, J. T. Fan, S. J. Xie, Y. Zhang, G. J. Mao and H. Wang, *Appl. Surf. Sci.*, 2022, **597**, 153686.
13 L. M. Rao, X. Y. Lu, L. L. Xu, Y. F. Zhu, T. Xue, Y. Ge, Z. S. Duan, X. M. Duan, Y. P. Wen and J. K. Xu, *Chemosphere*, 2022, **289**, 133116.
14 G. H. Jin, E. Ko, M. K. Kim, V. K. Tran, S. E. Son, Y. Geng, W. Hur and G. H. Seong, *Sens. Actuators, B*, 2018, **274**, 201–209.
15 C. H. Zhang, C. X. Chen, D. Zhao, G. Kang, F. N. Liu, F. Yang, Y. Z. Lu and J. Sun, *Anal. Chem.*, 2022, **94**, 3485–3493.
16 T. X. Yu, Y. F. Wang, K. Yuan, Q. Guo and J. Ge, *Sens. Actuators, B*, 2022, **367**, 132056.
17 F. P. Ran, Y. X. Xu, M. R. Ma, X. Y. Liu and H. X. Zhang, *Talanta*, 2022, **250**, 123702.
18 L. Zhang, Z. W. Liu, Q. Q. Deng, Y. J. Sang, K. Dong, J. S. Ren and X. G. Qu, *Angew. Chem., Int. Ed.*, 2021, **60**, 3469–3474.

19 Y. Y. Huang, J. S. Ren and X. G. Qu, *Chem. Rev.*, 2019, **119**, 4357–4412.
20 Y. Wei, S. Wu, Z. Q. Liu, J. S. Niu, Y. Zhou, J. S. Ren and X. G. Qu, *Mater. Today*, 2022, **56**, 16–28.
21 K. Dong, C. Xu, J. S. Ren and X. G. Qu, *Angew. Chem., Int. Ed.*, 2022, **61**, e202208757.
22 Z. Wang, Y. C. Zhang, X. Z. Wang and L. Han, *Biosens. Bioelectron.*, 2022, **206**, 114120.
23 X. Y. Wang, S. J. Dong and H. Wei, *Electroanalysis*, 2022, **34**, 1–13.
24 G. Y. Li, G. X. Wu, J. D. Huang, B. Wang, H. M. Li, W. Chen, J. T. Liang, M. X. Tan and Z. D. Zhou, *Bioelectrochemistry*, 2022, **147**, 108204.
25 D. Liu, C. H. Ju, C. Han, R. Shi, X. H. Chen, D. M. Duan, J. H. Yan and X. Y. Yan, *Biosens. Bioelectron.*, 2021, **173**, 112817.
26 Y. Q. Pei, L. J. Zeng, C. F. Wen, K. Wu, A. P. Deng and J. G. Li, *Mikrochim. Acta*, 2021, **188**, 194–194.
27 Y. X. Jia, S. Q. Zhao, Q. S. Qu and L. Yang, *Biosens. Bioelectron.*, 2022, **202**, 114020.
28 J. Y. Zhang and J. W. Liu, *Luminescence*, 2020, **35**, 1185–1194.
29 L. X. Yan, B. B. Wang, X. Zhao, L. J. Chen and X. P. Yan, *ACS Appl. Mater. Interfaces*, 2021, **13**, 60955–60965.
30 Q. J. Fu, X. B. Zhou, M. J. Wang and X. G. Su, *Anal. Chim. Acta*, 2022, **1216**, 339993.
31 F. Li, J. M. Jiang, H. Peng, C. X. Li, B. Li and J. B. He, *Sens. Actuators, B*, 2022, **369**, 132334.
32 Z. M. Li, X. L. Zhong, S. H. Wen, L. Zhang, R. P. Liang and J. D. Qiu, *Sens. Actuators, B*, 2019, **281**, 1073–1079.
33 J. Zhu, J. Pan, Y. C. Li, J. Yang and B. C. Ye, *Anal. Bioanal. Chem.*, 2022, **414**, 6271–6280.
34 S. Shariati and G. Khayatian, *New J. Chem.*, 2021, **45**, 21788–21794.
35 T. R. Bastami, M. Bayat and R. Paolesse, *Sensors*, 2022, **22**, 2072.
36 R. Saez-Hernandez, K. U. Antela, A. R. Mauri-Aucejo, A. Morales-Rubio and M. L. Cervera, *Food Chem.*, 2022, **389**, 133063.
37 J. Ge, L. K. Yang, Z. H. Li, Y. Wan, D. S. Mao, R. J. Deng, Q. Zhou, Y. Yang and W. H. Tan, *J. Hazard. Mater.*, 2022, **436**, 129199.
38 D. M. Liu, B. Xu and C. Dong, *TrAC, Trends Anal. Chem.*, 2021, **142**, 116320.
39 S. Melikishvili, I. Piovarci and T. Hianik, *Chemosensors*, 2021, **9**, 281.
40 M. L. Xue, W. Mao, J. S. Chen, F. F. Zheng, W. H. Chen, W. Shen and S. Tang, *Analyst*, 2021, **146**, 6726–6740.
41 Q. Q. Fan, Y. Gao, F. Mazur and R. Chandrawati, *Biomater. Sci.*, 2021, **9**, 6983–7007.
42 Q. Y. Liu, Q. Y. Jia, R. R. Zhu, Q. Shao, D. M. Wang, P. Cui and J. C. Ge, *Mater. Sci. Eng., C*, 2014, **42**, 177–184.
43 A. Hayat, W. Haider, Y. Raza and J. L. Marty, *Talanta*, 2015, **143**, 157–161.
44 X. Y. Wang and H. Wei, *J. Nanopart. Res.*, 2020, **22**, 22.
45 Z. W. Gan, T. Zhang, X. X. An, Q. Tan, S. J. Zhen and X. L. Hu, *Sens. Actuators, B*, 2022, **368**, 132181.
46 Z. F. Wang, Y. Liu, X. Y. Dong and Y. Sun, *ACS Appl. Mater. Interfaces*, 2021, **13**, 49974–49981.
47 Y. F. Liu, Y. H. Zhang, Q. Y. Liu, Q. Wang, A. Q. Lin, J. Luo, Y. Du, Y. W. Lin and H. Wei, *Analyst*, 2021, **146**, 1872–1879.
48 Z. Xu, L. Li, K. Li, M. L. Chen, J. Tu, W. Chen, S. H. Zhu and Y. H. Cheng, *Microchim. Acta*, 2021, **188**, 421.
49 M. Razavi, A. Barras, M. Ifires, A. Swaidan, M. Khoshkam, S. Szunerits, M. Kompany-Zareh and R. Boukherroub, *J. Colloid Interface Sci.*, 2022, **613**, 384–395.
50 S. Q. Li, D. Liu, B. Y. Wu, H. P. Sun, X. Y. Liu, H. X. Zhang, N. N. Ding and L. Wu, *Talanta*, 2022, **239**, 123088.
51 H. H. Ye, K. K. Yang, J. Tao, Y. J. Liu, Q. Zhang, S. Habibi, Z. H. Nie and X. H. Xia, *ACS Nano*, 2017, **11**, 2052–2059.
52 Z. J. Zhang, X. H. Zhang, B. W. Liu and J. W. Liu, *J. Am. Chem. Soc.*, 2017, **139**, 5412–5419.
53 Y. Jv, B. X. Li and R. Cao, *Chem. Commun.*, 2010, **46**, 8017–8019.
54 Y. F. Lee and C. C. Huang, *ACS Appl. Mater. Interfaces*, 2011, **3**, 2747–2754.
55 K. N. Han, J. S. Choi and J. Kwon, *Sci. Rep.*, 2017, **7**, 2806.
56 M. X. Mao, R. Zheng, C. F. Peng and X. L. Wei, *Biosensors*, 2020, **10**, 211.
57 B. W. Liu and J. W. Liu, *Nanoscale*, 2015, **7**, 13831–13835.
58 S. C. B. Gopinath, T. Lakshmipriya and K. Awazu, *Biosens. Bioelectron.*, 2014, **51**, 115–123.
59 L. Qiao, H. Wang, J. L. He, S. M. Yang and A. L. Chen, *Food Chem.*, 2021, **340**, 128181.
60 R. B. Liu, F. Y. Zhang, Y. X. Sang, M. X. Liu, M. H. Shi and X. H. Wang, *Foods*, 2022, **11**, 1802.
61 X. Y. Qi, Y. L. Zhao, H. P. Su, L. L. Wang, L. Li, R. Ma, X. C. Yan, J. A. Sun, S. Wang and X. Z. Mao, *Talanta*, 2022, **238**, 123032.
62 P. Weerathunge, R. Ramanathan, V. A. Torok, K. Hodgson, Y. Xu, R. Goodacre, B. K. Behera and V. Bansal, *Anal. Chem.*, 2019, **91**, 3270–3276.
63 R. Das, A. Dhiman, A. Kapil, V. Bansal and T. K. Sharma, *Anal. Bioanal. Chem.*, 2019, **411**, 1229–1238.
64 L. Li, R. Ma, Y. L. Zhao, L. L. Wang, S. Wang and X. Z. Mao, *Talanta*, 2022, **246**, 123534–123534.
65 Y. L. Zhao, L. Li, R. Ma, L. L. Wang, X. C. Yan, X. Y. Qi, S. Wang and X. Z. Mao, *Anal. Chim. Acta*, 2021, **1173**, 338710.
66 M. Alle, S. C. Park, R. Bandi, S. H. Lee and J. C. Kim, *Carbohydr. Polym.*, 2021, **253**, 117239.
67 M. Alle, R. Bandi, G. Sharma, R. Dadigala, S. H. Lee and J. C. Kim, *Int. J. Biol. Macromol.*, 2022, **201**, 686–697.
68 O. Adegoke, C. McKenzie and N. N. Daeid, *Sens. Actuators, B*, 2019, **287**, 416–427.
69 P. L. An, X. Xue, H. H. Rao, J. J. Wang, M. Gao, H. Q. Wang, M. Y. Luo, X. H. Liu, Z. H. Xue and X. Q. Lu, *Anal. Chim. Acta*, 2020, **1125**, 114–127.
70 T. R. Bastami and Z. Dabirifar, *RSC Adv.*, 2020, **10**, 35949–35956.

71 F. Amourizi and M. Ghaedi, *Polyhedron*, 2021, **210**, 115506.
72 E. Ko, W. Hur, S. E. Son, G. H. Seong and D. K. Han, *Microchim. Acta*, 2021, **188**, 382.
73 M. M. Shah, W. Ren, J. Irudayaraj, A. A. Sajini, M. I. Ali and B. Ahmad, *Sensors*, 2021, **21**, 8050.
74 K. V. Serebrennikova, N. S. Komova, A. N. Berlina, A. V. Zherdev and B. B. Dzantiev, *Chemosensors*, 2021, **9**, 332.
75 L. H. Jin, Z. Meng, Y. Q. Zhang, S. J. Cai, Z. J. Zhang, C. Li, L. Shang and Y. H. Shen, *ACS Appl. Mater. Interfaces*, 2017, **9**, 10027–10033.
76 W. Li, B. Chen, H. X. Zhang, Y. H. Sun, J. Wang, J. L. Zhang and Y. Fu, *Biosens. Bioelectron.*, 2015, **66**, 251–258.
77 X. X. Li, Q. W. Huang, W. Li, J. L. Zhang and Y. Fu, *J. Anal. Test.*, 2019, **3**, 277–285.
78 G. Chen, M. J. Jin, M. M. Yan, X. Y. Cui, Y. S. Wang, W. J. Zheng, G. X. Qin, Y. D. Zhang, M. J. Li, Y. Liao, X. Y. Zhang, F. Y. Yan, A. M. Abd El-Aty, A. Hacimuftuoglu and J. Wang, *Microchim. Acta*, 2019, **186**, 339.
79 M. M. Yan, G. Chen, Y. X. She, J. Ma, S. H. Hong, Y. Shao, A. M. Abd El-Aty, M. Wang, S. S. Wang and J. Wang, *J. Agric. Food Chem.*, 2019, **67**, 9658–9666.
80 Y. Fu, H. X. Zhang, S. D. Dai, X. Zhi, J. L. Zhang and W. Li, *Analyst*, 2015, **140**, 6676–6683.
81 W. Li, X. Zhi, J. J. Yang, J. L. Zhang and Y. Fu, *Anal. Methods*, 2016, **8**, 5111–5116.
82 Y. H. Sun, J. Wang, W. Li, J. L. Zhang, Y. D. Zhang and Y. Fu, *Biosens. Bioelectron.*, 2015, **74**, 1038–1046.
83 Y. Sun, R. X. Wang, X. Liu, G. Y. Shan, Y. W. Chen, T. Tong and Y. C. Liu, *Microchim. Acta*, 2018, **185**, 445.
84 Y. Lu, W. C. Ye, Q. Yang, J. Yu, Q. Wang, P. P. Zhou, C. M. Wang, D. S. Xue and S. Q. Zhao, *Sens. Actuators, B*, 2016, **230**, 721–730.
85 L. L. Wu, Z. J. Qian, Z. J. Xie, Y. Y. Zhang and C. F. Peng, *Chin. J. Anal. Chem.*, 2017, **45**, 471–475.
86 V. G. Panferov, N. A. Byzova, A. V. Zherdev and B. B. Dzantiev, *Microchim. Acta*, 2021, **188**, 309.
87 S. Singh, P. Tripathi, N. Kumar and S. Nara, *Biosens. Bioelectron.*, 2017, **92**, 280–286.
88 H. Liu, Y. Hua, Y. Y. Cai, L. P. Feng, S. Li and H. Wang, *Anal. Chim. Acta*, 2019, **1092**, 57–65.
89 H. Fang, S. N. Zhan, L. Feng, X. L. Chen, Q. Guo, Y. Q. Guo, Q. H. He and Y. H. Xiong, *Sens. Actuators, B*, 2021, **346**, 130368.
90 E. Ogut, C. Kip, B. Gokcal and A. Tuncel, *J. Colloid Interface Sci.*, 2019, **550**, 90–98.
91 A. Grau-Carbonell, S. Sadighikia, T. A. J. Welling, R. J. A. van Dijk-Moes, R. Kotni, M. Bransen, A. van Blaaderen and M. A. van Huis, *ACS Appl. Nano Mater.*, 2021, **4**, 1136–1148.
92 T. Feng, K. C. Chen, J. M. Zhong, Y. X. Cheng, H. L. Zhao and M. B. Lan, *Sens. Actuators, B*, 2022, **369**, 132265.
93 C. Kip, E. Akbay, B. Gokcal, B. O. Savas, M. A. Onur and A. Tuncel, *Colloids Surf., A*, 2020, **598**, 124812.
94 B. Yardimci, O. K. Koc, A. Uzer, J. Hizal and R. Apak, *Microchim. Acta*, 2021, **188**, 228.
95 M. Su, H. D. Chen, H. Zhang and Z. X. Wang, *Microchim. Acta*, 2022, **189**, 81.
96 W. Duan, Z. W. Qiu, S. F. Cao, Q. Guo, J. K. Huang, J. Y. Xing, X. Q. Lu and J. B. Zeng, *Biosens. Bioelectron.*, 2022, **196**, 113724.
97 Z. W. Qiu, W. Duan, S. F. Cao, T. Zeng, T. Y. Zhao, J. K. Huang, X. Q. Lu and J. B. Zeng, *Environ. Sci. Technol.*, 2022, **56**, 1713–1723.
98 X. Jiao, H. J. Song, H. H. Zhao, W. Bai, L. C. Zhang and Y. Lv, *Anal. Methods*, 2012, **4**, 3261–3267.
99 J. J. Lian, P. Liu, C. Q. Jin, Z. Q. Shi, X. L. Luo and Q. Y. Liu, *Microchim. Acta*, 2019, **186**, 1.
100 M. Q. Chi, Y. Zhu, Z. Z. Yang, M. Gao, S. H. Chen, N. Song, C. Wang and X. F. Lu, *Nanotechnology*, 2017, **28**, 295704.
101 M. Liu, Z. H. Li, Y. X. Li, J. J. Chen and Q. Yuan, *Chin. Chem. Lett.*, 2019, **30**, 1009–1012.
102 L. L. Fu, D. S. Yu, D. J. Zou, H. Qian and Y. H. Lin, *Molecules*, 2021, **26**, 6494.
103 B. Chishti, Z. A. Ansari, H. Fouad, O. Y. Alothman, M. Hashem and S. G. Ansari, *Crystals*, 2021, **11**, 178.
104 Y. R. Li, J. Wu, C. Zhang, Y. P. Chen, Y. Wang and M. X. Xie, *Microchim. Acta*, 2017, **184**, 2767–2774.
105 Z. Zhang, G. L. Xu, L. Xie and Y. P. Guan, *Microchim. Acta*, 2019, **186**, 581.
106 D. X. Dai, H. Y. Liu, H. Ma, Z. H. Huang, C. C. Gu and M. Z. Zhang, *J. Alloys Compd.*, 2018, **747**, 676–683.
107 Y. Y. Guo, L. Yan, R. Y. Zhang, H. Ren and A. H. Liu, *Process Biochem.*, 2019, **81**, 92–98.
108 Z. Lin, X. M. Zhang, S. J. Liu, L. L. Zheng, Y. M. Bu, H. H. Deng, R. T. Chen, H. P. Peng, X. H. Lin and W. Chen, *Anal. Chim. Acta*, 2020, **1105**, 162–168.
109 D. Q. Luo, X. H. Huang, B. Y. Liu, W. Y. Zou and Y. G. Wu, *J. Agric. Food Chem.*, 2021, **69**, 3537–3547.
110 T. R. Lin, L. S. Zhong, L. Q. Guo, F. F. Fu and G. N. Chen, *Nanoscale*, 2014, **6**, 11856–11862.
111 Z. Q. Xian, L. Zhang, Y. Yu, B. X. Lin, Y. M. Wang, M. L. Guo and Y. J. Cao, *Microchim. Acta*, 2021, **188**, 65.
112 L. P. Feng, L. X. Zhang, S. Chu, S. Zhang, X. Chen, Z. L. Du, Y. S. Gong and H. Wang, *Appl. Surf. Sci.*, 2022, **583**, 52496–52496.
113 Z. Q. Zhu, L. B. Gong, X. Y. Miao, C. Y. Chen and S. Su, *Biosensors*, 2022, **12**, 260.
114 Z. L. Lu, N. Lu, Y. Xiao, Y. Q. Zhang, Z. S. Tang and M. Zhang, *ACS Appl. Mater. Interfaces*, 2022, **14**, 11156–11166.
115 L. J. Huang, W. X. Zhu, W. T. Zhang, K. Chen, J. Wang, R. Wang, Q. F. Yang, N. Hu, Y. R. Suo and J. L. Wang, *Microchim. Acta*, 2018, **185**, 7.
116 A. Swaidan, A. Addad, J. F. Tahon, A. Barras, J. Toufaily, T. Hamieh, S. Szunerits and R. Boukherroub, *Anal. Chim. Acta*, 2020, **1109**, 78–89.
117 W. X. Zhang, X. P. Li, T. Y. Cui, S. C. Li, Y. Q. Qian, Y. Yue, W. Y. Zhong, B. Xu and W. Q. Yue, *Microchim. Acta*, 2021, **188**, 174.

118 X. J. Wu, T. M. Chen, J. X. Wang and G. W. Yang, *J. Mater. Chem. B*, 2018, **6**, 105–111.
119 L. J. Huang, Q. R. Zhu, J. Zhu, L. P. Luo, S. H. Pu, W. T. Zhang, W. X. Zhu, J. Sun and J. L. Wang, *Inorg. Chem.*, 2019, **58**, 1638–1646.
120 L. Lin, D. X. Chen, C. F. Lu and X. X. Wang, *Microchem. J.*, 2022, **177**, 107283.
121 Y. J. Song, X. H. Wang, C. Zhao, K. G. Qu, J. S. Ren and X. G. Qu, *Chem. – Eur. J.*, 2010, **16**, 3617–3621.
122 Y. J. Song, K. G. Qu, C. Zhao, J. S. Ren and X. G. Qu, *Adv. Mater.*, 2010, **22**, 2206–2210.
123 Y. Tao, Y. H. Lin, Z. Z. Huang, J. S. Ren and X. G. Qu, *Adv. Mater.*, 2013, **25**, 2594–2599.
124 H. Y. Sun, X. L. Liu, X. H. Wang, Q. S. Han, C. Qi, Y. M. Li, C. Wang, Y. X. Chen and R. Yang, *Microchim. Acta*, 2020, **187**, 110.
125 S. T. Zhang, H. Li, Z. Y. Wang, J. Liu, H. L. Zhang, B. D. Wang and Z. Y. Yang, *Nanoscale*, 2015, **7**, 8495–8502.
126 O. Adegoke, S. Zolotovskaya, A. Abdolvand and N. N. Daeid, *Talanta*, 2021, **224**, 121875.
127 P. K. Boruah and M. R. Das, *J. Hazard. Mater.*, 2020, **385**, 121516.
128 Z. R. Song, C. R. Jiang, F. Q. Wang, L. L. Yu, S. J. Ye, P. Dramou and H. He, *Mikrochim. Acta*, 2021, **188**, 207–207.
129 C. Peng, M. Y. Hua, N. S. Li, Y. P. Hsu, Y. T. Chen, C. K. Chuang, S. T. Pang and H. W. Yang, *Biosens. Bioelectron.*, 2019, **126**, 581–589.
130 O. Adegoke, S. Zolotovskaya, A. Abdolvand and N. N. Daeid, *Talanta*, 2020, **216**, 120990.
131 C. Liu, Y. M. Zhao, D. Xu, X. X. Zheng and Q. Huang, *Anal. Bioanal. Chem.*, 2021, **413**, 4013–4022.
132 Y. J. Wan, J. W. Zhao, X. C. Deng, J. Chen, F. N. Xi and X. B. Wang, *Front. Chem.*, 2021, **9**, 774486.
133 X. T. Zhao, S. Li, X. X. Yu, R. T. Gang and H. Wang, *Nanoscale*, 2020, **12**, 21440–21446.
134 Y. Z. Shen, Y. L. Wei, Z. M. Liu, C. Nie and Y. W. Ye, *Microchim. Acta*, 2022, **189**, 233.
135 Y. F. Fan, W. C. Zhang, Y. M. Liu, Z. X. Zeng, X. Quan and H. M. Zhao, *ACS Appl. Mater. Interfaces*, 2019, **11**, 17467–17474.
136 N. C. Cheng, S. Stambula, D. Wang, M. N. Banis, J. Liu, A. Riese, B. W. Xiao, R. Y. Li, T. K. Sham, L. M. Liu, G. A. Botton and X. L. Sun, *Nat. Commun.*, 2016, **7**, 13638.
137 J. Liu, M. G. Jiao, L. L. Lu, H. M. Barkholtz, Y. P. Li, Y. Wang, L. H. Jiang, Z. J. Wu, D. J. Liu, L. Zhuang, C. Ma, J. Zeng, B. S. Zhang, D. S. Su, P. Song, W. Xing, W. L. Xu, Y. Wang, Z. Jiang and G. Q. Sun, *Nat. Commun.*, 2017, **8**, 15938.
138 X. B. Zhou, M. K. Wang, J. Y. Chen, X. L. Xie and X. G. Su, *Anal. Chim. Acta*, 2020, **1128**, 72–79.
139 Y. Mao, S. J. Gao, L. L. Yao, L. Wang, H. Qu, Y. Wu, Y. Chen and L. Zheng, *J. Hazard. Mater.*, 2021, **408**, 124898.
140 L. P. Sun, C. Li, Y. Yan, Y. Yu, H. Zhao, Z. J. Zhou, F. Wang and Y. Feng, *Anal. Chim. Acta*, 2021, **1180**, 33856.
141 W. J. Jing, X. K. Cui, F. B. Kong, W. Wei, Y. C. Li, L. Z. Fan and X. H. Li, *Analyst*, 2021, **146**, 207–212.
142 B. Liu, Y. T. Xue, Z. Y. Gao, K. R. Tang, G. Wang, Z. B. Chen and X. Zuo, *Colloids Surf., B*, 2021, **208**, 112060.
143 F. Honarasa, F. Peyravi and H. Amirian, *J. Iran. Chem. Soc.*, 2020, **17**, 507–512.
144 H. Ren, L. Yan, M. J. Liu, Y. B. Wang, X. Liu, C. Y. Liu, K. Liu, L. X. Zeng and A. H. Liu, *Sens. Actuators, B*, 2019, **296**, 126517.
145 L. J. Zhao, Z. P. Wu, G. N. Liu, H. Y. Lu, Y. Gao, F. M. Liu, C. G. Wang, J. W. Cui and G. Y. Lu, *J. Mater. Chem. B*, 2019, **7**, 7042–7051.
146 Q. Q. Zhu, Y. H. Yuan, B. Yan, J. Zhou, J. L. Zuo and L. J. Bai, *Analyst*, 2021, **146**, 7284–7293.
147 N. Cheng, C. Z. Zhu, Y. L. Wang, D. Du, M. J. Zhu, Y. B. Luo, W. T. Xu and Y. H. Lin, *J. Anal. Test.*, 2019, **3**, 99–106.
148 L. Liang, Y. J. Huang, W. R. Liu, W. Y. Zuo, F. G. Ye and S. L. Zhao, *Front. Chem.*, 2020, **8**, 671.
149 M. H. Ying, G. Z. Yang, Y. J. Xu, H. L. Ye, X. Lin, Y. Lu, H. B. Pan, Y. Bai and M. Du, *Analyst*, 2021, **147**, 40–47.
150 Q. T. Li, Q. Wang, Y. Li, X. D. Zhang and Y. M. Huang, *Anal. Methods*, 2021, **13**, 2066–2074.
151 X. L. Zhao, J. L. Liu, F. T. Xie, T. Yang, R. Hu and Y. H. Yang, *Spectrochim. Acta, Part A*, 2021, **262**, 120117.
152 N. Nataraj, T. W. Chen, Z. W. Gan, S. M. Chen, M. R. Hatshan and M. A. Ali, *Mater. Today Chem.*, 2022, **23**, 100725.
153 F. P. Ran, Y. X. Xu, M. R. Ma, X. Y. Liu and H. X. Zhang, *Talanta*, 2022, **250**, 123702.

